1-1-2011

ENU-3 is a novel outgrowth and guidance protein in c. elegans

Callista Stephanie Yee
Ryerson University

ENU-3 IS A NOVEL OUTGROWTH AND GUIDANCE PROTEIN

IN *C. ELEGANS*

By

Callista Stephanie Yee

BSc., Biomedical Science, University of Waterloo, 2009

A thesis

presented to Ryerson University

in partial fulfillment of the

requirements for the degree of

Master of Science

in the Program of

Molecular Science

Toronto, Ontario, Canada, 2011

I hereby declare that I am the sole author of this thesis or dissertation.

I authorize Ryerson University to lend this thesis or dissertation to other

institutions or individuals for the purpose of scholarly research.

Callista Stephanie Yee

I further authorize Ryerson University to reproduce this thesis or dissertation

by photocopying or by other means, in total or in part, at the request of other

institutions or individuals for the purpose of scholarly research.

Callista Stephanie Yee

ENU-3 is a novel axon outgrowth and guidance protein in *C. elegans*. MSc. 2011.

Callista Stephanie Yee, Molecular Science, Ryerson University.

Abstract

During the development of the nervous system, the migration of many cells and axons is guided by extracellular molecules. These molecules bind to receptors at the tips of the growth cones of migrating axons and trigger intracellular signalling to steer the axons along the correct trajectories. Previous work has identified a novel mutant, *enu-3* (enhancer of Unc), that enhances the motor neuron axon outgrowth defects observed in strains of *Caenorhabditis elegans* that lack either the UNC-5 receptor or its ligand UNC-6/Netrin. *enu-3* single mutants have weak motor neuron axon migration defects. Both outgrowth defects of double mutants and axon migration defects of *enu-3* mutants were rescued by expression of the H04D03.1 gene product. ENU-3/H04D03.1 encodes a novel predicted putative trans-membrane protein of 204 amino acids. ENU-3 is expressed weakly expressed in many cell bodies along the ventral cord, including those of the DA and DB motor neurons.

<u>Acknowledgments</u>

Table of Contents

List of Tables

List of Figures

List of Abbreviations

BLAST	Basic Local Alignment Search Tool
CED	Cell Death
DCC	deleted in colorectal cancer
DNA	deoxyribonucleic acid
dsRNA	Double-stranded ribonucleic acid
Dpy	Dumpy
DTC	distal tip cell
EFN	Ephrin
EMS	ethyl methylsulfonate; ethyl methanesulfonate
ENU	Enhancer of Uncoordinated
GEI	GEX interacting protein
GEX	Gut on the EXterior
GFP	green fluorescent protein
NGM	Nematode growth media
PCR	polymerase chain reaction
PLX	Plexin
Robo	Roundabout
RNA	Ribonucleic acid
RNAi	ribonucleic acid interference
SMP	Semaphorin
SNP	single nucleotide polymorphism
SRC	Sarcoma
TGF-β	transforming growth factor β
UNC	Uncoordinated
Wnt	Wingless
ZEN	Zygotic Enclosure Defective

Chapter 1: General Introduction

1.1　　　General introduction and outline of thesis

The nervous system in multicellular eukaryotes develops in a stereotypical fashion. The nervous systems of humans are comprised of over a trillion neuronal connections that are wired in a similar manner in every individual. Neurons initially begin as a single cell (soma) which may migrate from its birthplace to its final position. Once there, it can send out projections (axons) towards a specific target cell. The tips of growing axons, growth cones, extend small filamentous structures known as filopodia. These filamentous structures sample the environment and are influenced to grow in a specific path by chemo-attraction or repulsion by guidance cues. Amazingly, cells are able to make decisions regarding growth and form connections between adjacent and distant target cells alike in a stereotypical fashion. However, relatively little is known about how these decisions are made and what factors play a role in directing these growing axons. Some of the questions that developmental neurobiology attempt to answer are: What are the molecular cues required for guidance of developing neurons? What is the chronological and spatial organization of these cues and their receptors? How do these interactions effect growth of the developing neurons? I have attempted to answer some of these questions by studying axon guidance using a genetic approach in the free living nematode *Caenorhabditis elegans*. The conservation of axon guidance signalling pathways between both vertebrates and invertebrates makes *C. elegans* an ideal model organism.

In *C. elegans*, dorsal-ventral guidance of many neurons as well as other cells of mesodermal origin has been shown to be partially dependent on the Netrin/UNC-6 signalling pathway. UNC-6 interacts with two receptors, UNC-5 and UNC-40, which mediate repulsion and attraction respectively (Hedgecock et al., 1990). These mutants were originally isolated and

1

described as <u>unc</u>oordinated and thus the corresponding affected genes were given the designation *unc*. However, null mutants of each of these three proteins yields only partial penetrance of axon guidance defects of the dorsally directed motor neurons, indicating that there must be other pathways working redundantly with the UNC-6/Netrin pathway to control dorsal guidance of neurons. My thesis work has involved characterization of a novel protein, ENU-3 (<u>en</u>hancer of <u>u</u>ncoordinated), which was identified through a genetic enhancer screen in a genetic background lacking the UNC-5 receptor. Double mutants of both ENU-3 and UNC-5 have significantly increased DA/DB motor axon outgrowth defects, where the axons fail to leave the cell body.

In Chapter 1, I present an introduction to axon guidance, an overview of the *C. elegans* hermaphrodite nervous system and various signalling pathways that have been studied in *C. elegans* and other model organisms. In Chapter 2, I provide the materials and methods that I used to conduct my study. In Chapter 3, I present the results of my findings. Lastly, in Chapter 4, I present a discussion of my results and propose future experiments. Hopefully this work will contribute to the further understanding of the pathways involved in axon guidance in both *C. elegans* and humans alike.

1.2 *Caenorhabditis elegans* **as a model organism**

C. elegans is a well characterized model organism that has been used extensively to study the molecular basis of gene and protein function in eukaryotes. *C. elegans* is a free living soil nematode that exists usually as a hermaphrodite with some males, allowing for robust genetics that generally follow Mendelian principles. The adult hermaphrodite is approximately 1 mm in length and has a generation time of 3 days at 20°C, giving rise to approximately 300 progeny. *C.*

elegans can be easily cultivated in the laboratory, either on solid or liquid media. They live a 'plush' life in the laboratory, where they are fed bountiful amounts of *E. coli* and require only trace metals and cholesterol. Thus, *C. elegans* strains are quite inexpensive to breed and can be easily scaled up depending on the application (Brenner, 1974).

The life cycle of *C. elegans* begins as an egg. After hatching, progeny mature through four larval stages (L1-L4) after which they develop to become young adults and finally adults. Adult wild-type hermaphrodites have the ability to live for approximately 20 days. *C. elegans* prefer ambient temperatures but have the ability to enter an alternative phase in their life cycle during L2 called dauer in times of hardship and lack of favourable living conditions. During this dauer period most metabolic processes besides essential ones are shut off. Once their needs are sufficiently met, the worms will leave the dauer stage as young adults and resume their normal lifestyle (Brenner, 1974).

C. elegans was first introduced as a tool to study genetics by Sydney Brenner in 1974 and over 450 *C. elegans* laboratories exist worldwide. Extensive studies using various forms of microscopy and serial sectioning have mapped the entire cell lineage and neuronal connectivity in *C. elegans* (White et al., 1986).

The *C. elegans* genome is composed of 6 chromosomes, containing approximately 97 megabases of genetic information that encode 19,735 protein-coding genes (Hillier et al., 2005). Although this genome size may seem large, it is quite small in comparison to the human genome which is composed of 23 chromosomes coded by 3 billion bases that encode 20,000-25,000 genes. *C. elegans* was one of the first eukaryotic organisms to have its genome entirely sequenced, which was completed in 2002. An up-to-date genetic map and various bioinformatics

online tools such as WormBase (www.wormbase.org) are freely available to *C. elegans* scientists. Scientists are able to take advantage of the sensitivity of the germ-line of the hermaphrodites and use certain mutagens such as EMS (ethyl methyl sulfonate), TMP (trimethyl phosphate), and UV to generate mutations and create mutants for unidentified genes or for specific genes, depending on the approach. A reverse genetics technique has been employed by the Worm Knockout Consortium with the goal of generating deletion mutants for every single gene in the *C. elegans* genome in order to determine the role of every worm protein.

1.3　　Structure and function of neurons

Neurons can be arguably described as both complex and simple structures simultaneously. A simple neuron is composed of a cell body, dendrites, and an axon (Figure 1.1). Despite its simplicity in terms of structure, these cells are able to receive information and transmit and pass along information to their targets over long distances. The neuron receives input from other cells via stimulation of the dendrites, which are long, highly branched structures. In turn, the stimulation generates a differential of membrane potential which passes through the structure of the neuron. This ionic potential generates an action potential, which is a self-propagating wave of electrical potential that begins at the axon hillock and is transmitted through a single, long elongated process known as the axon. The axon then innervates its target and releases a neurotransmitter that provides a specific signal to elicit the desired response in the target post-synaptic cell or neuron. In humans, the distance between neuronal cell bodies and their targets can be greater than 1 metre long, thus complex and accurate guidance cues directing the axonal growth cone are crucial for proper connectivity.

1.4   The nervous system of *C. elegans*

Since the complete connectivity of the nervous system is known in *C. elegans*, it is an ideal organism for studying mechanisms of axon guidance and outgrowth. Being aware of the connectivity allows researchers to perform laser ablation and genetic analysis studies to determine the pathways that are responsible for axon guidance. The adult hermaphrodite has 302 neurons which are located between the hypodermis and the basal lamina. Due to the simple shape of the worm, neurons typically run longitudinally or circumferentially along the hypodermis, depending on their function and type. Three different classes of neurons exist: motor neurons, sensory neurons and interneurons (White et al., 1986).

Most of the neurons present in *C. elegans* are found bundled in the nerve ring which encircles the pharynx, and two longitudinal nerve cords found along the dorsal and ventral midline. The nerve ring acts as the brain of the worm and is the site of many neuronal synapses. The ventral nerve cord (VNC) extends from the head to the tail of the worm and is composed of left and right bundles. The VNC contains processes of sensory ganglia, interneurons, as well as 57 motorneurons. Motorneurons send out commissures laterally or circumferentially depending on the target muscle. The motorneurons that extend their axons circumferentially to the dorsal midline then proceed to turn longitudinally to form the other longitudinal nerve cord, the dorsal nerve cord (DNC) (Figure 1.2) (White et al., 1986).

There are eight classes of motorneurons, DA, DB, DD, AS, VD, VA, VB, and VC which innervate body wall muscles through neuromuscular junctions to enable forward and backward movements of the worm (Chalfie et al., 1985). The DA, DB and DD neurons are formed during embryogenesis while the others are formed during the L1 stage (White et al., 1986). The DA, DB, DD and AS classes of neurons send commissures dorsally, innervating dorsal body wall muscles

(Figure 1.2). The VA, VB, VD and VC classes send commissures ventrally, running along the ventral nerve cord and innervating ventral body wall muscles (Figure 1.2) (White et al., 1986). Laser ablation experiments have shown that the DB and VB motorneurons are excitatory and stimulate muscle contractions to result in forwards movement while the DA and VA motorneurons are also excitatory and allow for stimulation to result in backwards movement. Further studies have shown that the DD and VD motorneurons are inhibitory and cause relaxation of the muscles (Chalfie et al., 1985). A- and B- type motorneurons are cholinergic (which utilize acetylcholine) whereas D- type motorneurons are GABAergic (which utilize ɣ-aminobutyric acid). Interestingly, the VC motorneurons express multiple transmitters including both acetylcholine and ɣ-aminobutyric acid (Hall & Altun, 2008).

1.5   Growth cones and Axon Guidance

During development, the end of the growing axon is known as the growth cone (Reviewed in Maskery & Shinbrot, 2005). The growth cone possesses the ability to sample the environment by extending finger-like microfilament projections known as filopodia and lamellipodia (Figure 1.3). These projections, depending on the stimulus and the proteins present on the projections, physically orient the growth cone and thus subsequently guide the axon to its target destination. It has been shown that growth cones are still able to extend their projections when their corresponding axon has been severed, indicating that growth cones do not require the soma and possess all of the molecular machinery to make navigational decisions (Campbell & Holt, 2001). Previous studies investigating axon guidance have shown that there are multiple pathways that are responsible for directing axonal growth cones. If severing the axons of the growth cones still

allow for filopodia extension, then the growth cones themselves must possess the machinery to allow for cytoskeletal rearrangement (Shaw & Bray, 1977).

There are four general mechanisms of axon guidance: target-derived diffusible chemo-attractive and-repulsive cues and contact-dependent attractive and repulsive cues (Tessier-Lavigne & Goodman, 1996). The Semaphorins and Ephrins are examples of short-range repulsive cues which are able to generate boundaries or areas that inhibit axon migration (Wang et al., 1999; Wong et al., 1997). The UNC-6/Netrins and their associated proteins are examples of secreted cues that are able to behave as either long-range chemoattractive or chemorepulsive cues (Ishii et al., 1992). In *C. elegans*, axons are able to grow circumferentially along the dorsal-ventral axis or longitudinally along the anterior-posterior axis (White et al., 1986). Genes controlling the circumferential guidance have been well characterized, such as the UNC-6/UNC-5/UNC-40 pathway. These proteins have been shown to mediate axon migration as well as other cell migrations on the hypodermis of *C. elegans* (Hedgecock et al., 1990).
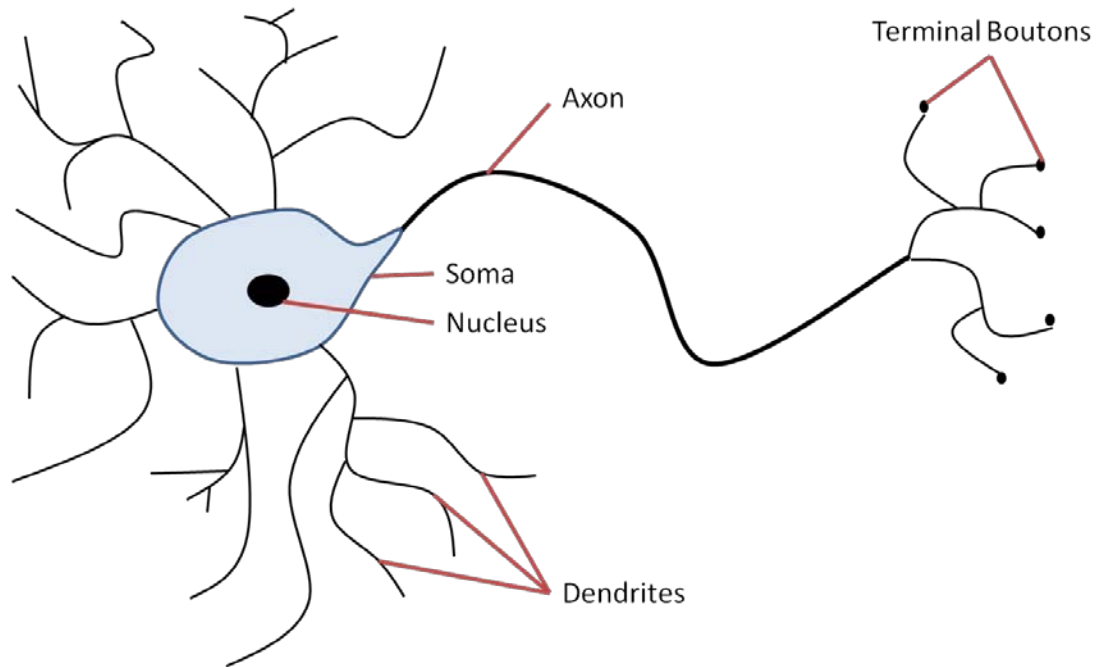
Figure 1.1: A simple cartoon of a neuron.

Neurons are structures that generally consist of a single cell known as a soma. Branch-like

structures known as dendrites receive input from other neurons. Neurons extend a long arm like

projection known as an axon which can extend up to metres in length in some organisms. At the

end of the axon, terminal boutons synapse onto its target cell.

Figure 1.2: A subset of nerves found in *C. elegans* with their normal trajectories.

The major longitudinal tracts are found in the lateral, sublateral and subdorsal positions (White et

al., 1986).
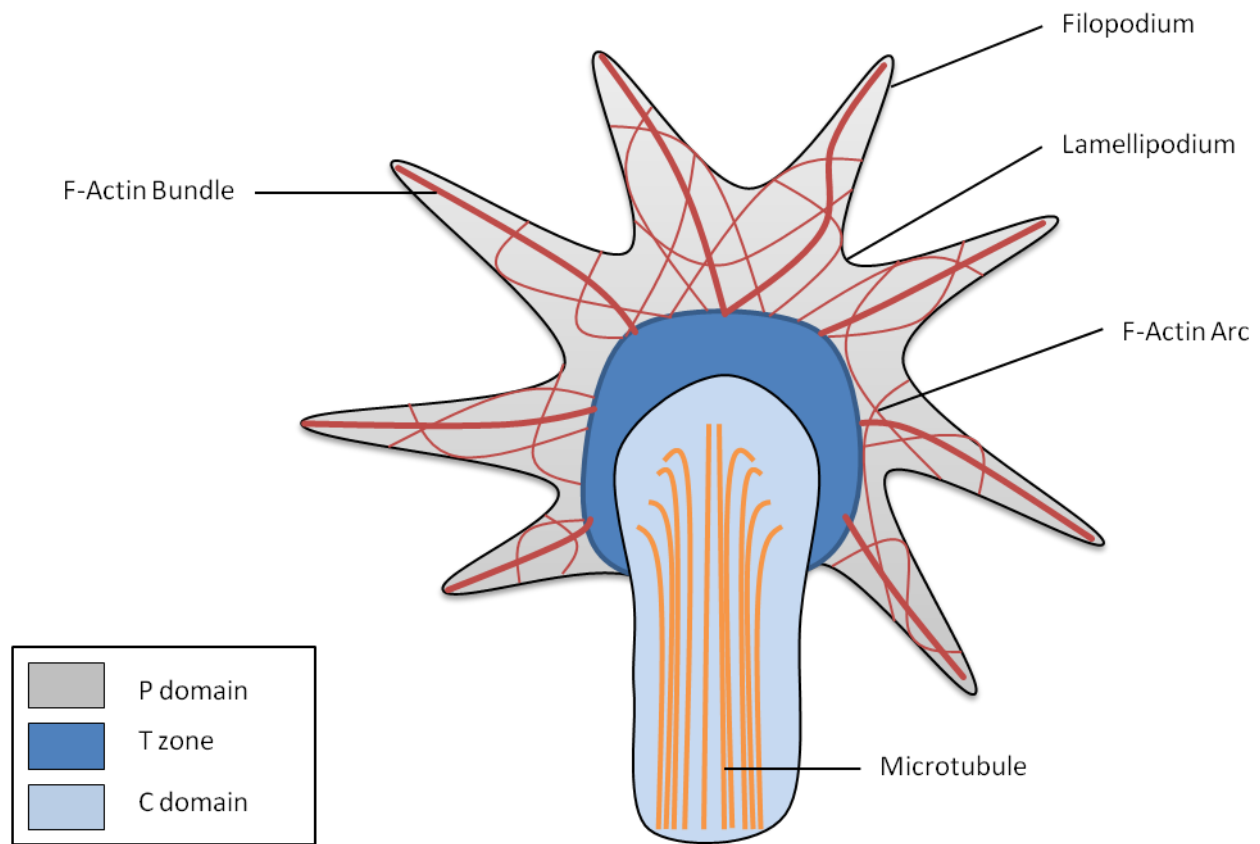
Figure 1.3: A growth cone of a developing axon.

The growth cone consists of three different structural areas, including the P domain, the T zone and the C domain. At the tip of the growth cone, finger like projections known as filopodium extend out and sample the environment (after Maskery & Shinbrot, 2005).

1.6 The UNC-6/Netrin Signalling Pathway

The UNC-6/Netrin signalling pathway has been shown to be conserved throughout nematodes and vertebrates alike and plays a major role in cell and axon migrations. UNC-6 is a laminin-related secreted cue which was first identified in *C. elegans* where it affects growth cone and cell migration along the dorsal-ventral axis (Hedgecock et al., 1990; Ishii et al., 1992). UNC-6 homologues were also found to instruct axonal growth in *Drosophila* (Harris, et al., 1996) and vertebrates (Serafini et al., 1994).

The UNC-6 signalling pathway involves interactions between the secreted cue, UNC-6, and two receptors, UNC-5 and UNC-40/DCC/Frazzled. UNC-6 is expressed from cells located on the ventral side of the worm and its expression probably decreases dorsally in a gradient fashion. UNC-5 and/or UNC-40 are present on growth cones of developing axons and the receptors are either repelled or attracted to the source of UNC-6 respectively, resulting in dorsal or ventral migration respectively. However, some axons can express both UNC-5 and UNC-40 on their growth cones. In this case, the repulsive effect caused by UNC-5 is suspected to overcome the attractive effect of UNC-40 and resulting in dorsal movement (Colamarino & Tessier-Lavigne, 1995; Hong et al., 1999) (Figure 1.3).

The receptors for UNC-6 are both single pass transmembrane receptors. Cells and neurons expressing UNC04/DCC/Frazzled are attracted to UNC-6 (Chan et al., 1996). Cells and neurons expressing UNC-5 are repelled by UNC-6 (Leung-Hagesteijn et al., 1992). Mutants for all three of these proteins exhibit similar defects with respect to cell and axon migrations. The mutants have a moderate to severe uncoordinated (Unc) phenotype which is attributed to errors that occur during dorsal migration of motor axons. As mentioned previously, the DA, DB, DD, VD and AS classes of motorneurons project commissures circumferentially towards dorsal muscle from cell

11

bodies which lie on the VNC. Examination of these motorneurons in *unc-6*, *unc-5* and *unc-40* putative null mutants have shown that some of these neurons fail to send out commissures or have commissures that are mostly severely misguided and do not reach their usual targets (Hedgecock et al., 1990).
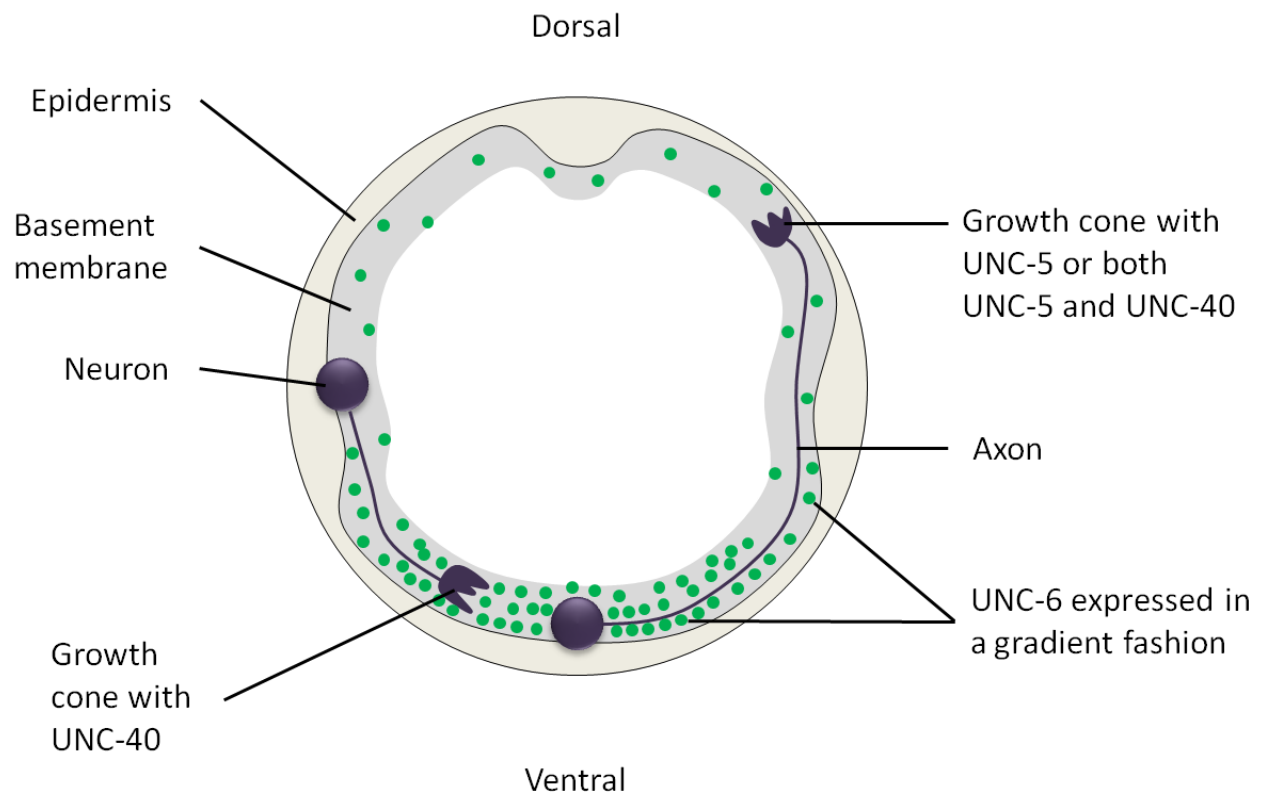
Figure 1.4: A Cross-section model of UNC-6 signalling in the *C. elegans* body wall.

UNC-6 is expressed by cells in the ventral region. Axons that express UNC-5 or UNC-5 and

UNC-40 on their growth cones are repelled by the source of UNC-6 whereas axons that express

UNC-40 on their growth cones are attracted to the ventral sources of UNC-6 (After Wadsworth,

2002).

Another characteristic of *unc-6, unc-5,* and *unc-40* mutants is the failure of the dorsal migration component of the distal tip cells (DTC) (Figure 1.4) and the male linker cell (MLC) during gonadogenesis (Hedgecock et al., 1990). These two cells of mesodermal origin are found at the leading edge of the gonad that migrate during development of the female (DTC) or male (MLC) sexual organs. Both sexes of *C. elegans* exhibit longitudinal migration and circumferential migration during elongation of the developing gonad. In hermaphrodites, the DTC migrates from a position close to the vulva in the ventral mid-body. It first migrates along the ventral side, stalls and then makes a second migration towards the dorsal side. Once there, it turns again and finally migrates back towards the vulva on the dorsal side. The gonads in the mutants fail to complete the circumferential migration and instead migrate back towards the vulva on the ventral side. This forces the gut to be pushed to one side and causes what appear to be clear patches along the ventral side of the body of the worm. These clear patches are called distal tip cell defects or DTC defects (Figure 1.4). It has been shown that UNC-5 expression is co-incident with the second phase of the migration (Su et al., 2000; Killeen et al., 2002). As observed with the motor axon migration defects, *unc-40* null mutants have fewer DTC defects than *unc-6* and *unc-5* null mutants (Figure 1.4) (Hedgecock et al., 1990; Chan et al., 1996).

UNC-6 and UNC-40 but not UNC-5 are involved in guiding migrations in the ventral direction. *unc-6* and *unc-40* mutants exhibit axon guidance defects of a subset of neurons which are positioned laterally and send commissures ventrally to enter the VNC. The neurons that are affected are the axons of the mechanosensory neurons (AVM, PVM and PDE), sensory neurons (PHA and PHB) and the HSN motorneurons. Some of the commissures of the affected axons migrate longitudinally instead of ventrally and consequently do not reach the VNC (Figure 1.5) (Hedgecock et al., 1990; Desai et al., 1998).

Interestingly, null mutants for each of the three genes do not result in complete penetrance of any of the phenotypes described, indicating that there must be redundancy and other pathways working along with the Netrin/UNC-6 pathway to control dorsal guidance (Hedgecock et al., 1990; Chan et al., 1996). Another interesting observation is that the penetrance of the defects varies depending on the position of the cells affected. For example, the DTC migration defects appear to be far more penetrant in the posterior gonad arm versus the anterior arm despite their identical structure and mirroring (Hedgecock et al., 1990). The reason for this difference is not yet understood.
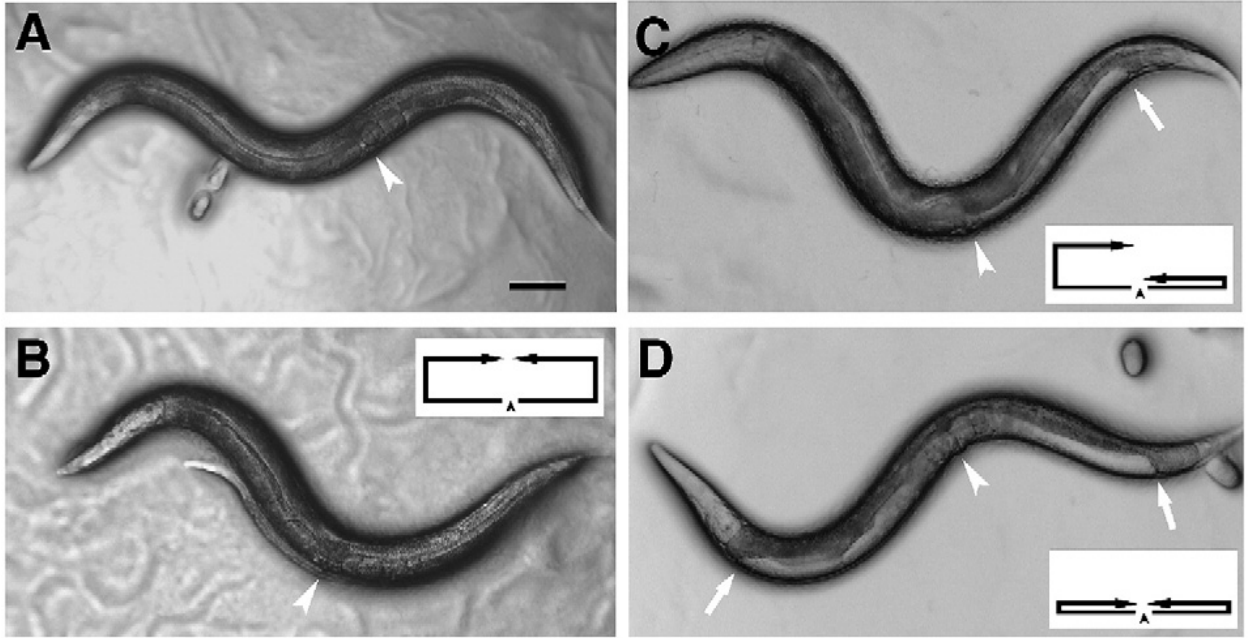
Figure 1.5: A comparison of wild type (N2) distal tip cell migration to *unc-5(e53)* mutants. Frames A and B represent wild type DTC migration. Frame C shows an animal with a distal tip cell defect in the posterior gonad, while frame D illustrates migration failure in both the anterior and posterior gonad arms (Zheng et al., 2007). Scale bar = 30 microns. The white arrow pointing at the mid body indicates the location of the vulva, while the arrows at the proximities of the animal indicate distal tip cell defects.

TGF-β/UNC-129 was first identified in a screen aimed at finding suppressors of ectopic

UNC-5 (Colavita & Culotti, 1998). UNC-129 is expressed in the DA/DB motorneurons, the

VNC and in the dorsal muscle band. UNC-129 expression follows a gradient opposite to UNC-6,

such that UNC-129 is highly expressed on the dorsal side of the animal and its expression

decreases ventrally (Figure 1.5) (Colavita et al., 1998). It has been shown recently that TGF-β

/UNC-129 facilitates long-range repulsive guidance of Netrin/UNC-6 by enhancing UNC-5 +

UNC-40 signalling and interacting directly with UNC-5 in order to inhibit UNC-5 alone

signalling (MacNeil et al., 2009). This expression is important to allow for long range guidance

of the motorneurons. UNC-40 signalling is also important for long-range migrations of motor

neurons in *Drosophila* (Mrkusich et al., 2010).

1.7   Other Axon Guidance Signalling Pathways

Although the main focus of my thesis is related to dorsal guidance, I will briefly discuss

other axon guidance mechanisms in *C. elegans*. The growing axons, depending on their

trajectory, express receptors which behave in a manner dependent on the axon guidance cues

expressed in the environment through which the axon is migrating. Similarly, migrating cells

may also express receptors for these ligands and migrate in a direction based on these cues. In *C.

elegans*, guidance cues generally emanate and function in guidance of migrations in either the

dorsal-ventral or anterior-posterior direction (Figure 1.5). In the dorsal-ventral signalling, UNC-

6/Netrin is expressed in cells located in the ventral regions and SLT-1/Slit and UNC-129/TGFB

are expressed in cells in the dorsal regions. In anterior-posterior signalling, SLT-1/Slit is

expressed in cells located in the of anterior regions during embryogenesis and EGL-20/Wnt is

expressed in cells located in posterior regions (Killeen & Sybingco, 2008). Ephrins and

Semaphorins have also been shown to play a role in axon guidance and morphogenesis.

1.7.1 Ventral Guidance

Although UNC-6/Netrin has been determined to be involved in ventral migration in *C.*

elegans, a separate pathway mediated by SLT-1/Slit also plays a role in ventral guidance. Slit

and its receptor Robo (Roundabout) were first described in *Drosophila* and appear to be

phylogenically conserved across vertebrates and invertebrates (Hao et al., 2001; Long et al.,

2004). The *C. elegans* version, of Slit/SLT-1, is expressed dynamically and was found to be

expressed within the anterior muscles of the worm during embryogenesis and in dorsal muscle

later on during development (Ito et al., 2001). As a result, SLT-1 generates a gradient along the

anterior-posterior axis of the worm. SLT-1 has a single receptor, SAX-3, with homology to Robo

(Zallen et al., 1998). The gradient which is generated functions chemorepulsively, such that

neurons that express SAX-3 are repelled by the source of SLT-1. SAX-3 is also expressed in the

growth cones of the AVM and PVM mechanosensory neurons. These cell bodies, as mentioned

earlier, are positioned longitudinally and their axons migrate in the ventral direction to join the

VNC and then in an anterior direction towards the nerve ring (Figure 1.7, Figure 1.8). The

migration of the axons in the ventral direction thus can be attributed to repulsion away from

dorsal muscle elicited by SLT-1 working through SAX-3 and the attraction towards the VNC by

UNC-6 working though UNC-40 (Hao et al., 2001).

It has been shown recently that only two pathways are implicated in ventral guidance of the

AVM neuron (Figure 1.8). In the absence of both the UNC-6 and the SLT-1 pathways, ventral

18

guidance of the AVM does not occur and the axon migrates along mid body towards the head (Hao et al., 2001). Interestingly, a recent publication by Fujisawa et al. (2007) has shown that a novel protein, EVA-1, has the ability to bind to SLT-1 as well as SAX-3. The authors proposed that in the absence of either EVA-1 or SLT-1, SAX-3 binds to UNC-40 and prevents UNC-40 from binding to UNC-6. This binding of UNC-40 prevents UNC-6 signalling from occurring and in turn shuts down ventral guidance altogether as both pathways are unable to function.

1.7.2   Anterior Posterior Guidance

Both the UNC-6/Netrin and SLT-1/Slit pathways play a role in anterior-posterior guidance of neurons in the worm (Hedgecock et al., 1990, Hao et al., 2001). Mutants for genes involved in these pathways frequently have anterior-posterior guidance defects of the ALM and PLM axons, as well migration defects of the Q cell derived neurons. A diagram depicting the lineage and trajectories of the cells that originate from the Q cells is shown in Figure 1.6. In *C. elegans*, Wnts play a major role in mediating axon outgrowth, cell migration, cell fate and cell polarity. Wnt cues usually emanate from the posterior portion of the worm (Figure 1.5) (Pan et al., 2006). Cells and axons that express Frizzled receptors are repelled by the Wnts and thus move in the anterior direction towards the head (Hilliard et al., 2006). In *C. elegans*, there are five Wnts (EGL-20, LIN-44, CWN-1, CWN-2, MOM-2) and four Frizzleds (MOM-5, CFZ-2, MIG-1, LIN-17) (Reviewed in Killeen and Sybingco, 2008).
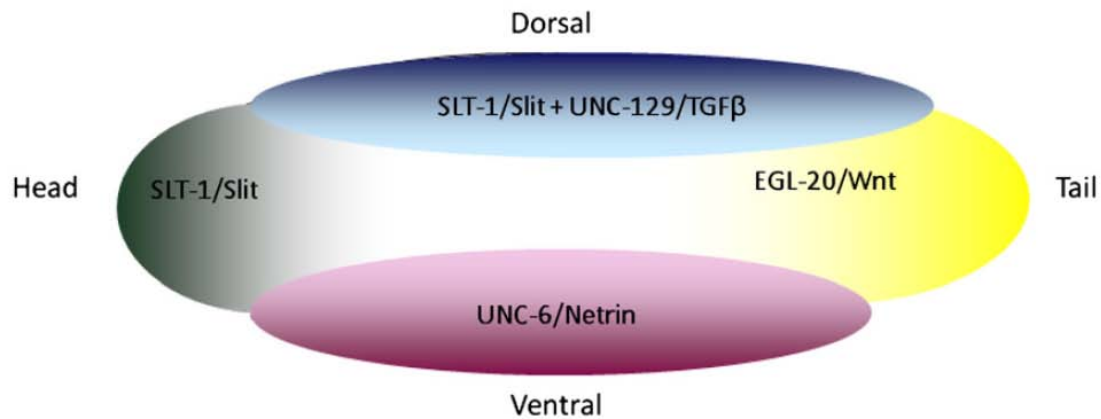
Figure 1.6: Major axon guidance cues in *C. elegans*.

These guidance cues not only affect neuronal guidance, but cell migration of many other structures as well. UNC-6/Netrin is expressed by cells located in the ventral regions where it repels axons expressing UNC-5 or attracts axons expressing UNC-40. UNC-129 acts to mediate long range guidance of the DA and DB motorneurons by promoting UNC-5/UNC-40 signalling at the expense of UNC-5 homodimers (MacNeil et al., 2009). SLT-1/Slit is expressed in dorsal muscle and repels axons that express SAX-3 and functions both in the dorsal-ventral direction and in the anterior-posterior direction (Hao et al., 2001). EGL-20/Wnt and other Wnts are expressed from cells of posterior origin. Cells that express Frizzled receptors are repelled by Wnts and thus move in the anterior direction (Killeen and Sybingco 2008).
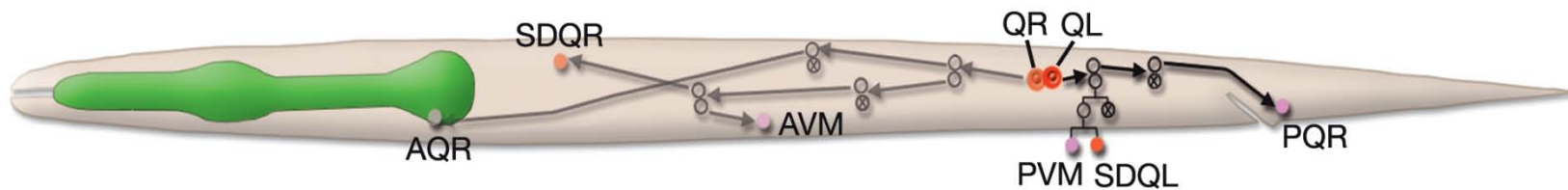
Figure 1.7: The lineage and trajectories of the neurons that arise from the Q neuroblast cells.

The Q cells originate in the posterior half of the animal and give rise to neurons that migrate both in the anterior-posterior and dorsal-ventral direction. *unc-40* mutants frequently have Q cell migration defects, such that the PVM is misplaced and is located in the anterior half of the animal, beside the AVM or ALM cell bodies (Hobert, 2010).
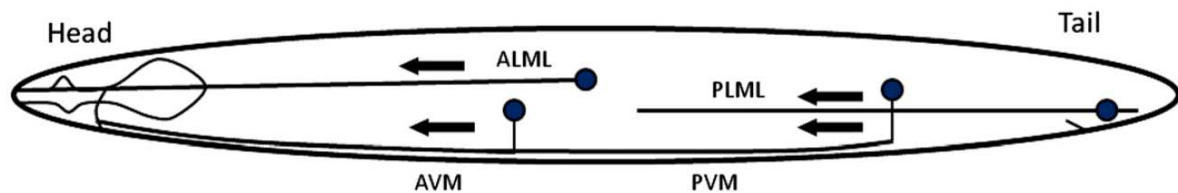
Figure 1.8: Schematic of four of the six mechanosensory neurons in *C. elegans*.

The two missing mechanosensory neurons are ALMR and PLMR, the counterparts of ALML

and PLML which lie on the right side of the worm. The ALM and PLM neurons send out axons

which migrate in an anterior direction towards the head. The AVM is located on the right side of

the body and the PVM is located on the left side of the body. Both the AVM and PVM have

axons that migrate ventrally and then in an anterior direction towards the head (Killeen and

Sybingco 2008).

1.7.3   Semaphorins

Other mechanisms besides the Netrin/UNC-6, Slit/SLT-1 and Wnt pathways have been

identified which play roles in both axon guidance and epithelial morphogenetic cell movements.

The Semaphorins are a conserved family of guidance cues that were first identified in

grasshoppers for their role in axon guidance and fasciculation (Kolodkin et al., 1992).

Semaphorin signalling appears to repel growth cone migration by inhibiting integrin-mediated

adhesion and causing disruption of the local tubulin and actin cytoskeleton (Tran et al., 2007). It

has also been shown that Semaphorin signalling can affect the local translation of cytoskeletal

components within the migrating growth cone (Campbell & Holt, 2001). However, some

members of the Semaphorin family have also been reported to attract growth axons (Wong et al.,

1997; Bagnard et al., 1998).

In *C. elegans*, semaphorin signalling involves three Semaphorins (SMP-1, SMP-2 and

MAB-20) and two Plexins (PLX-1 and PLX-2) (Roy et al., 2000). SMP-1 and SMP-2 are class I

semaphorins and they act semi-redundantly to signal to a type A Plexin (PLX-1), affecting male

ray tail positioning and vulval morphogenesis (Fujii et al., 2002; Dalpe et al., 2004).

MAB-20, which is a secreted class II Semaphorin, has been shown to bind to a type B Plexin

(PLX-2) and it affects epidermal morphogenesis and axon guidance (Roy et al., 2000; Nakao et

al., 2007). MAB-20 mutants have severe morphological defects, such as hypocontraction, ray

fusion defects and split tails. These defects can be mainly attributed to misalignment of

microfilaments during elongation. MAB-20 mutants also have weak axon guidance and

fasciculation defects in the DA /DB class motorneurons, suggesting a role in dorsal-ventral

guidance. Cell migration defects of the PVM touch neuron were also observed, where a third of

the MAB-20 mutant animals have the PVM cell body located near or anterior to the mid-body

instead of lying in the middle of the posterior half of the animal. These positioning defects

suggest a problem with anterior-posterior guidance. Interestingly, MAB-20 mutants also exhibit

DTC migration defects, where in 9% of the animals the DTCs undergo additional turns,

indicating that MAB-20 may be required to prevent the DTCs from turning beyond their normal

stopping points (Roy et al., 2000).

1.7.4   Ephrins

Another family of signalling ligands known to play a role in morphogenesis and neuronal

development is the Ephrin family. Ephrins are cell-surface-tethered ligands which are either

tethered by a glycosylphosphatidylinositol (GPI) group (type A) or by a transmembrane region

(type B) and act by juxtracrine signalling. Ephrins act as ligands for receptors known as Eph

receptors or EphRs. EphRs are currently the largest known family of receptor tyrosine kinases

(RTKs). RTKs are transmembrane proteins that have an extracellular domain (to receive input)

and an intracellular kinase domain (to transmit input) (Palmer & Klein, 2003). Interestingly,

Ephrin signalling can function in a forward and reverse fashion. Forward Ephrin signalling

involves an Ephrin binding an Eph receptor, while reverse signalling involves an Ephrin

signalling into the cytosol of ephrin-exposing cell backwards (Murai & Pasquale, 2003).

Both classes of receptors act together with Ephrins to create distinct boundaries,

ultimately affecting cell migration through a repulsion mechanism. A single gene with homology

with EphR has been found in *C. elegans* called *vab-1*. VAB-1 mutants were characterized based

on their "variably abnormal" morphology which includes variable embryonic and larval lethality,

a notched head and other defects (Brenner, 1974). Four type A Ephrins have been identified

24

through the *C. elegans* genome sequencing project, termed *efn-1*, *efn-2*, *efn-3* and *efn-4*. EFN-1, EFN-2 and EFN-3 have been shown to interact with and signal to VAB-1 (Wang et al., 1999). However, mutations in *efn-4* appear to act synergistically with mutations in *vab-1* and *efn-1*, suggesting that EFN-4 functions independently of VAB-1 during morphogenesis. It was also shown that *efn-4* mutations do not synergize with *mab-20* mutations, suggesting that EFN-4 and Semaphorin II signalling lie in the same or opposing pathways during neuronal embryogenesis (Chin-Sang et al., 2002)

1.8 Hypothesis

Prior to my arrival at Ryerson, a genetic enhancer screen was conducted aimed at finding new motor axon guidance genes (Sybingco, 2008). The purpose of the screen was to identify new genes that work to affect motor axon guidance in a pathway parallel to the UNC-6/Netrin pathway. The screen was conducted in an *unc-5(e53)* (a null) background. Five mutants that enhanced axon outgrowth defects of the DA and DB motor neurons in *unc-5(e53)* were isolated (Sybingco, 2008; Naqvi, 2009). Subsequent analysis of the motor axons in one mutant, *enu-3 (rq1)*, showed that mutants exhibit severe motor axon outgrowth defects in *enu-3(rq1);unc-5(e53)*. In addition *enu-3* mutants have mild motor axon guidance defects. ENU-3 appears to be a novel axon guidance molecule and it apparently functions in a pathway parallel to the UNC-6/Netrin pathway for axon outgrowth.

1.9   Specific Objective of Thesis Work

The objective of my research was to genetically characterize *enu-3* mutants and determine the function of ENU-3 and establish its role in development of the nervous system. Extensive genetic and phenotypic characterization was performed and various molecular techniques were employed to characterize the two available alleles of *enu-3*. Expression of various rescue and reporter constructs were performed in order to confirm the molecular identity of *enu-3* and to visualize the expression pattern of ENU-3.

Chapter 2. Materials and Methods

2.1   Handling of Worm Strains:

All strains were maintained and handled at 20°C as previously described (Brenner, 1974). Bristol N2 was designated as the wild-type strain (Brenner, 1974). The mutants that were used in this study include: LG I: *unc-40(e1430)*; LG II: *clr-1(e1745ts)*; LG III: *enu-3(rq1)*, *enu-3(tm4519)*; IV: *unc-5(e53)*, *unc-5(e152)*, *dpy-20(e1282);* LG V: *him-5(e1490)*, X: *unc-6(e78)*, *unc-6(ev400)*, *slt-1(eh15)*. Strains were kept at 16°C for short to medium term storage and frozen at -80°C for long term storage.

2.2   Genetic Crosses:

All crosses were performed at 20°C with the exception of any crosses with *clr-1(e1745ts)*. Instead, crosses were performed at 16°C to allow for permissive mating. Crosses were typically performed by crossing *him-5(e1420); dpy-20(e1282)* males in order to generate F_1 males of one of the mutants to be crossed. The resulting F_1 males were crossed with the second strain and usually 10 of the resulting F_1 heterozygote hermaphrodites were picked onto individual 4 cm plates. Hermaphrodites were allowed to self fertilize and the resulting progeny were screened for F_2 hermaphrodites which appeared to have visual traits of both parental mutants. Approximately 10 of the putative cross-progeny were picked and followed clonally for at least 3 generations to ensure homozygosity. All genetic crosses were performed under typical dissecting microscopes at 40x magnification. An epifluorescence dissection microscope (Leica, model MZFLIII) was used on occasion to detect the presence of transgenes in cross progeny.

2.3   Transgenes

The following transgenes were used in this study: *evIs82b*, *unc-47p::gfp, mec-7::gfp,*

enu-3::enu-3, enu-3p::gfp, enu-3p::enu-3::gfp, unc-129p::enu-3::gfp

Array Name	Reporter Type	Expression	Reference
evIs82b	Transcriptional Fusion (*unc-129p::gfp; dpy-20*)	Ventral nerve Cord, DA and DB motorneurons, seam cells	Colavita et al., 1998
oxIs12	Transcriptional Fusion (*unc-47p::gfp; dpy-20*)	DD and VD motorneurons	McIntire et al., 1997
muIs32	Transcriptional Fusion (*mec-7p::gfp*)	Mechanosensory neurons	Ackley et al., 2001
rqEx1	Rescue Construct (*enu-3(+); myo-2::yfp*)	-	This study
rqEx2	Transcriptional Fusion (*enu-3p::gfp; myo-2::yfp*)	Ventral Nerve Cord, motorneurons, unidentified tail neurons, PVT	This study
rqEx3	Translational Fusion (*enu-3p::enu-3::gfp*)	Ventral Nerve Cord, motorneurons, unidentified tail neurons, PVT	This study
rqEx4	Cell Autonomy Construct (*unc-129p::enu-3::gfp; myo-2::yfp*)	Ventral nerve Cord, DA and DB motorneurons, seam cells	This study

Table 2.1: A list of extrachromosomal arrays and integrated transgenes used in this study.

2.4 Polymerase Chain Reaction (PCR)

The polymerase chain reaction method was performed using Taq polymerase in order to A) confirm the presence of a deletion within *enu-3(tm4519)* and to B) amplify DNA for reporter and rescue constructs. A typical PCR reaction consists of an initial denaturing step, followed by 25-30 cycles of denaturing, annealing, and extension. Once the cycles were complete, a final extension was performed and the reaction was complete. All steps were performed as according to manufacturers' instructions. Annealing temperatures and extension times were approximated based on primer annealing temperatures and amplicon sizes. Exact conditions are listed in Chapter 5 (Supplementary Information).

2.5 Isolation of RNA and cDNA Preparation

RNA was isolated using a TRIzol (Invitrogen, USA) based method from L4 animals. L4 animals were picked into DEPC (diethylpyrocarbonate) treated water (Fisher Scientific, USA) and treated with chloroform (Invitrogen) and TRIzol as described by manufacturer's instructions. Isopropanol was used to precipitate the RNA and the pellet was washed with 70% ethanol (made with DEPC treated water).

cDNA (complimentary deoxyribonucleic acid) was generated using the RNA (ribonucleic acid) pellets using standard methods. A first strand synthesis kit (GE Healthcare, USA) was obtained as a gift from Dr. Homayoun Vaziri (Ontario Cancer Institute) and RNA was prepared as per manufacturer's instructions. The resulting cDNA was heated at 68°C to denature the cDNA/RNA duplex. cDNA concentrations were measured using a spectrophotometer (230 nm) (Biorad, Canada) and appropriate dilutions were made to perform PCR reactions using equal amounts of template of the strains that were to be tested. Various reactions were performed using

the SL1 and SL2 primers and primers specific for the *enu-3* gene (Supplementary Table 1). PCR

reactions were performed with TaKaRa ExTaq (Takara Biotech Inc., Japan) and were analyzed

on 2-2.5% agarose gels.

2.6 Construction of Reporter Constructs and Microinjection

Through SNP mapping and fosmid and PCR product injection, a single gene, H04D03.1,

was shown to be sufficient to rescue the defects observed in *enu-3(rq1);unc-5(e53)*. The

following method was performed in order to generate various rescue constructs and to determine

the expression pattern of H04D03.1.

The construction of the rescue construct pMK300 was described previously (Naqvi,

2010). This rescue construct contained a cloned copy of H04D03.1 which included 3 kb

upstream of H04D03.1, the H04D03.1 gene product and 1 kb of the *unc-54* 3'UTR (which

stabilizes mRNA in the nervous system)(Fire Lab Vector Kit, Addgene). This construct was

injected into *enu-3(rq1)* mutants (30 ng/uL) with *myo-2::yfp* (70 ng/uL) as a co-injection marker.

The resulting extrachromosomal array was given the designation *rqEx1*.

Construction of reporter constructs were generated using a polymerase chain reaction

fusion method as described previously (Hobert, 2002). A 1.8 kb fragment encoding green

fluorescent protein (GFP) and the *unc-54* 3'UTR was amplified from pPD95.75 using GFP

specific primers (5'-AGC-TTG-CAT-GCC-TGC-AGG-TCG-3' and 5'- AAG-GGC-CCG-TAC-

GGC-CGA-CTA-3').

A transcriptional fusion construct was generated by amplifying 3 kb of the promoter of

H04D03.1 and fusing it to a fragment encoding GFP (Refer to Section 6.1 of the Supplementary

Materials). The forward primer binds 3 kb upstream and the reverse fusion primer binds

approximately 100 bp upstream of the initiator ATG. This fragment was amplified using Long Template Expand System 2(Roche) and was fused to the GFP reporter amplicon using TaKaRa Ex Taq Polymerase (Takara Biotech Inc.). This construct was injected into *him-5;dpy-20* mutants (30 ng/uL) with *myo-2::yfp* (70 ng/uL) as a co-injection marker. The resulting extrachromosomal array was given the designation *rqEx2*.

Similarly, a translational fusion construct was generated by amplifying the H04D03.1 promoter and gene and fusing it to a fragment encoding GFP (Refer to Section 6.2 of the Supplementary Materials). The translational fusion used the same forward primer as the transcriptional fusion, but differs with respect to the reverse primer since the primer binds immediately before the stop codon of H04D03.1. This fragment was amplified LongAmp Taq Polymerase (New England Biolabs) and was fused to the GFP reporter amplicon using TaKaRa Ex Taq Polymerase (Takara Biotech Inc.). This construct was injected into *him-5;dpy-20* mutants (30 ng/uL) with *dpy-20(+)* (70 ng/uL) as a co-injection marker. The resulting extrachromosomal array was given the designation *rqEx3*.

In order to address the question of cell autonomy, the H04D03.1 gene product was driven by the *unc-129* promoter. 2.5 kb of this promoter is sufficient to drive expression in the DA and DB motorneurons but not the dorsal muscle band (Colavita et al., 1998). The promoter was amplified from pAC12 using the outside and fusion primers (Refer to Section 6.3 of the Supplementary Materials). Using the translational fusion as a template, the primer H04D03.1::GFP forward primer and the nested GFP primer was used to amplify a DNA fragment containing the H04D03.1 gene fused to GFP. This amplicon was then fused to the *unc-129* promoter and microinjected at approximately 30ng/uL with 70ng/uL of *myo-2p::yfp*. The resulting extrachromosomal array was designated *rqEx4*.

Microinjection of mutants was performed at the Samuel Lunenfeld Research Institute at Mt. Sinai Hospital in Toronto, Ontario. Young adults were mounted onto 0.5% agarose pads supplemented with a drop of halocarbon oil and were microinjected on a Zeiss Axiovert 10 microscope using instrumentation purchased from Sutter Instruments. The total concentration of DNA that was microinjected into the animals was kept at approximately100 ng/uL. Successfully injected worms were transferred to a 4 cm plate and rinsed with M9 to remove residual oil. Animals were allowed to self fertilize and the resulting F_1 generation was screened for transgenic animals.

2.7 Scoring of DA and DB Motorneuron Defects

The DA and DB motorneurons were visualized using the *evIs82b* transgene, which encodes a transcriptional reporter (2.5 kb of *unc-129*) driving GFP. This transgene is expressed in select DA and DB motor neurons but not the dorsal muscle band (Colvavita et al., 1998). As described previously, the DA and DB motorneurons migrate from the ventral cord circumferentially to the dorsal side of the animal where they then turn and innervate their target muscles. All animals were scored at the L4 stage. There were three main phenotypes that were scored using this reporter transgene: axon outgrowth, axon migration/fasciculation and axon guidance.

Axon outgrowth defects have been well characterized in other neurons but have not been previously examined in detail in the DA and DB motor neurons. Motor neurons were considered outgrowth defective if there was no apparent axon leaving the cell body. It can be argued that there is axon outgrowth and that the axons are in fact leaving the cell bodies but are migrating

along the ventral cord. However, we were unable to make this distinction due to technical limitations and these axons were considered axon outgrowth defective.

Motor neuron axon migration and fasciculation defects are defined as fusions of the axon or crossing over each other. This phenotype occurs predominantly in the VD and DD neurons but occurs infrequently in the DA and DB motorneurons. Axons were scored based on defective migrations and all axons were accounted for. No cell bodies produced extra axons.

Axon guidance defects were scored as described by MacNeil et al. (2009). The DA and DB motorneurons in certain genetic backgrounds, notably UNC-6 pathway mutants, have defects where the motorneurons have proper outgrowth but turn and migrate aberrantly. Guidance defects were grouped into two main categories: short range defective and long range defective. Axons were considered short range defective if the axons turned aberrant before the midline of the animal, which is marked by the seam cells. Axons that turned aberrant after the midline of the animal were considered long range defective. The *evIs82b* transgene has "leaky" expression and is weakly expressed in the seam cells, so this facilitated determination of short or long range axon migration defects.

Chi squared tests were employed to test significance. Significance is reported below each figure. Each double mutant is compared relative to the single mutant background, which is introduced as the preceding value in each table.

2.8 RNAi (RNA Interference)

RNAi procedures were performed as previously described by using the Ahringer clone library (Fraser et al., 2000). RNAi clones were cultured in 5 mL of LB media overnight at 37°C

and spread in a confluent layer over standard RNAi plates (Fraser et al., 2000). Plates were allowed to grow for overnight at room temperature and stored at 4°C until use. Approximately 20-30 L4 synchronized animals were plated onto the RNAi clone plates and were allowed to self fertilize and give rise to F1s. 20-30 L1s were transferred in a similar manner to another set of RNAi plates and were allowed to self fertilize and give rise to F2s. L4 F2s were then picked and scored for the appropriate phenotype.

2.9   Scoring of Distal Tip Cell Defects

In a normally developing hermaphrodite, the gonad arms migrate in a U-shape, where they migrate along the anterior-posterior axis from the vulva in midbody, turn 90 degrees to move dorsally, and finally migrate back towards the vulva again but on the dorsal side to complete the U. However, in UNC-6 pathway mutants, the gonad migrates aberrantly and during the second stage of the migration, where the DTC migrates ventral to dorsal, often resulting in a ventral clear patch. The migration of the developing gonad is led by the distal tip cell. Depending on the cues impinging on the receptors present on the distal tip cell, guidance of the gonad can be affected. In order to determine if ENU-3 plays a role in distal tip cell migration, L4/young adult animals were mounted on 2% agarose pads and examined under 400x with an upright microscope using DIC optics. Animals were considered DTC defective if the gonad failed to complete the first 90 degrees turn from ventral to dorsal.

Chapter 3.   Results

A visual enhancer screen was conducted in an *unc-5(e53)* background in order to identify mutants in genes that work parallel to the UNC-6/Netrin pathway in the guidance of the DA and DB motor neurons out of their cell bodies in the ventral cord. Standard EMS mutagenesis followed by visual microscopic analysis of animals expressing *unc-129::gfp (evIs82b)* was performed. Five independent mutants were eventually isolated from the screen. Three mutants were mapped using "snip-SNP" analysis on the *C. elegans* genome using PCR and primers that generate products digestable by DraI (Sybingco, 2008). One mutant known by the allele name *rq1* was mapped to chromosome III around 2.5 map units. *rq1* and a second allele *tm4519* were later called *enu-3.* The characterization of the two alleles of *enu-3, (rq1)* and *(tm4519)*, are presented in this section.

In order to determine which gene in the region corresponds to the gene mutated in *rq1* rescue experiments using wild-type copies of genes that map to the region where *rq1* was mapped were conducted (Bueno de Mesquita, 2008; Naqvi, 2009). Wild-type copies of fosmids, cosmids and individual genes around the region where the *rq1* allele was mapped were microinjected into *enu-3(rq1);unc-5(e53)* to effect rescue of the motor axon outgrowth defects, scored using *evIs82b*. It was determined that *enu-3* corresponds to a novel gene of unknown function called H04D03.1 (Bueno de Mesquita 2008; Naqvi, 2009) at +2.5 map units on linkage group III. The gene is 1117 bases in size (including introns) and has three exons (Figure 3.1).
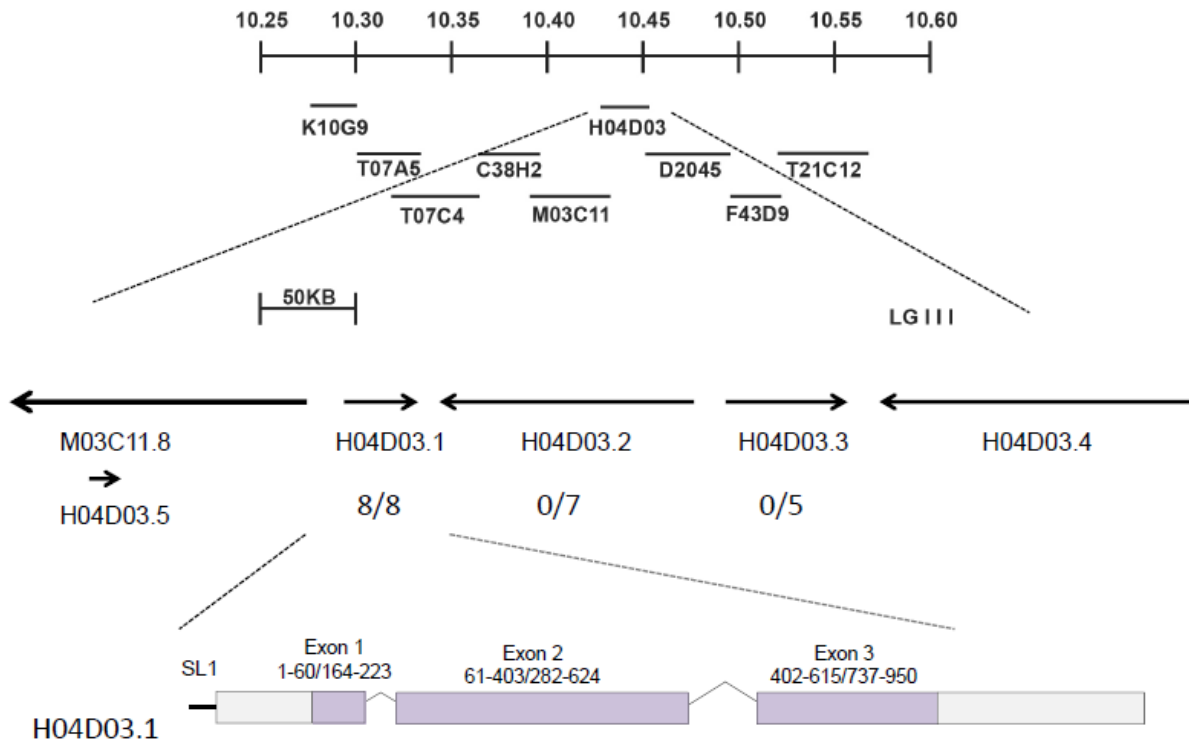
Figure 3.1: A schematic depicting the position of H04D03.1/ENU-3 on the genome. H04D03.1 is trans-spliced to SL-1. The numbers depict the number of rescued lines constructed. H04D03.1 has 3 exons and is located on chromosome 3 at +2.5 map units.

3.1   **ENU-3 enhances axon outgrowth of UNC-5 and UNC-6 double mutants**

unc-5(e53) single mutants have axon outgrowth defects, where DA/DB motorneuron cell bodies fail to produce an axon, or the axon runs along the ventral nerve cord and does not migrate circumferentially as expected. However, the penetrance of the axon outgrowth defects in the single mutant is low, suggesting that there are other genes involved in circumferential axon outgrowth besides those of the UNC-6/Netrin pathway. From the EMS screen reported previously, a mutant known as *rq1* was shown to enhance the axon outgrowth defects of *unc-5(e53)*. This double mutant, *enu-3(rq1);unc-5(e53)*, had approximately double the percentage of overall axon outgrowth defective animals of *unc-5(e53)* alone (Table 3.1. Figure 3.2). More specifically, axons of DB4, DB5 and DB6 neurons were most significantly affected. Interestingly, *enu-3(tm4519);unc-5(e53)* mutants exhibited enhanced penetrance of axon outgrowth defects in most of the axons examined relative to *enu-3(rq1)*. The double mutant of *unc-5(e53)* with *enu-3(tm4519)* had less defects in terms of percentage of animals affected relative to the single mutant, but displayed a much higher frequency of defects across all of the DA and DB motorneurons, relative to *enu-3(rq1);unc-5(e53)* which primarily affected only three of the DB cell bodies. This difference can be attributed to the fact that *tm4519* is a presumptive null allele and that *rq1* is likely to be a hypomorphic allele of *enu-3*.

In order to further support the idea that *enu-3* functions in the UNC-6/Netrin pathway, double mutants were constructed with different alleles of *unc-6*. A putative *unc-6* null strain, *unc-6(ev400)*, had similar axon outgrowth defects to *unc-5(e53)* and *enu-3(rq1);unc-6(ev400)* had an enhancement of the axon outgrowth defects (Table 3.1). The affected axons in this double mutant were DB5 and DB6. The outgrowth defects in DB5 were close to those seen in *enu-3;unc-5(e53)*. Since both alleles of *enu-3* enhanced the outgrowth defects of *unc-6(ev400)*, it

supports the idea that *enu-3* functions parallel to the UNC-6/Netrin pathway. However, when a hypomorphic allele of *unc-6* was scored, *unc-6(e78)*, the mutant, to our surprise, showed higher axon outgrowth defects than *unc-6(ev400)* in outgrowth of DB4 and DB5. The double mutant between *unc-6(e78)* and *enu-3(tm4519)* was constructed and there was a slight enhancement of the axon outgrowth defects in DB5 (from 49% to 58%) over that observed in *unc-6(e78)* alone.

Thus, based on the genetic interactions with the two different alleles of *enu-3* with UNC-6/Netrin pathway mutants, it can be concluded that *enu-3* appears to function parallel to UNC-5 and UNC-6 and is at least partially responsible for the axon outgrowth of the DA and DB motorneurons.

Animals lacking the second UNC-5 receptor, UNC-40, have no axon outgrowth defects at all. In order to understand axon outgrowth further, we next tested whether lack of BOTH UNC-5 and UNC-40 altered the motor axon outgrowth defects (Table 3.1). We found to our surprise that the motor axon outgrowth defects were LESS in the *unc-40(e1430);unc-5(e53)* double mutant than in *unc-5(e53)* alone while *unc-40(e1430)* had no motor axon outgrowth defects at all. A triple mutant lacking UNC-40, ENU-3 and UNC-5 enhanced the outgrowth defects of the *unc-40(e1430);unc-5(e53)* but the defects were lower than the *enu-3;unc-5(e53)* doubles (Table 3.1). The defects in the triple mutant were similar to those of *unc-6(ev400).* Therefore, the full effect of ENU-3 on axon outgrowth requires the presence of UNC-40, but ENU-3 also has UNC-40 independent defects that may also be UNC-6 independent.
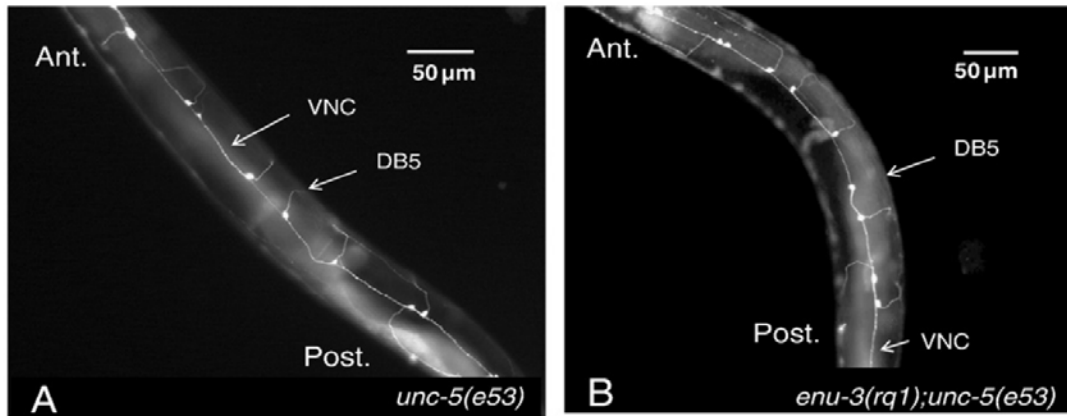
Figure 3.2: *enu-3* enhances the motor axon outgrowth defects of *unc-5(e53)*.

A) An example of a *unc-5(e53)* mutant and B) an *enu-3(rq1);unc-5(e53)* mutant at 400x

magnification showing the ventral cord and the motor neurons exiting. The animals are rolled

over on the slide so that the ventral nerve cord is facing upwards. Arrows indicate the ventral

nerve cord (VNC) and the DB5 soma.

	DB3	DA3	DB4	DA4	DB5	DA5	DB6	DA6	DB7	DA7	%	n
unc-5(e53)	0	3	6	2	10	2	6	0	0	0	27	100
enu-3(rq1);unc-5(e53)	3	2	14^b	1	19^b	1	13^b	0	0	0	50^c	100
enu-3(tm4519);unc-5(e53)	8	16^c	30^c	18^c	32^c	4	32^c	2	1	2	40^b	100
enu-3(rq1/tm4519);unc-5(e53)	5	9^c	14^b	5	17^b	2	12^a	2	0	0	36	84
unc-6(ev400)	0	1	2	1	17	1	3	0	0	0	36	100
enu-3(rq1);unc-6(ev00)	0	0	9	2	31^c	3	10^b	0	2	0	51^a	100
enu-3(tm4519);unc-6(ev400)	5	2	9	2	32^c	2	5	0	2	0	51^a	130
unc-6(e78)	0	0	28	0	49	0	4	0	0	0	41	102
enu-3(tm4519);unc-6(e78)	0	0	26	0	58	3	7	1	0	0	52	95
unc-40(e1430);unc-5(e53)	0	0	3	0	2	0	2	0	0	0	5	100
unc-40(e1430);enu-3(tm4519);unc-5(e53)	2	1	9	1	16	1	9	0	1	0	300	100

Table 3.1: The *enu-3* mutations enhance the motor neuron axon outgrowth defects of *unc-5* and *unc-6* mutants in the DA and DBs. The percentage of animals with cell bodies in the ventral cord without axons exiting the ventral cord was scored for the strains shown. The % indicates % animals affected with the mutant phenotype (a indicates *p* value on a chi test of 0.05, b means a *p* value of 0.01, c means a *p* value of less than 0.001).

3.2   *enu-3* **mutants have weak axon migration defects**

As mentioned previously, the *enu-3(rq1)* allele was recovered from a genetic enhancer screen as a double mutant with *unc-5(e53)*. Once the *unc-5(e53)* background was removed, the single mutant was examined and was found to have mild axon migration defects. Axon migration defects, in the context of this work, were defined as axon's crossing over each other or fusion defects of the motor axons (Figure 3.3). In N2, these defects are relatively uncommon and only occur in 4% of the population (Table 3.2). However, in *enu-3(rq1)* and *enu-3(tm4519)* mutants, there are a significantly increased percentage of axon migration defects where the most affected axons are DA3, DB4 and DA5. DA3 and DB4 tended to exhibit axon crossing over defects or tended to fuse together past the mid body region (Table 3.2) (as marked by the seam cells in Figure 3.3). Interestingly, DA5 was found to cross over with DB5 in *enu-3(rq1)*, but seemed more likely to crossover with DB6 in *enu-3(tm4519)*. These defects have been well characterized and observed in the VD and DD motorneurons but have not been well characterized and observed in the DA and DB motorneurons.
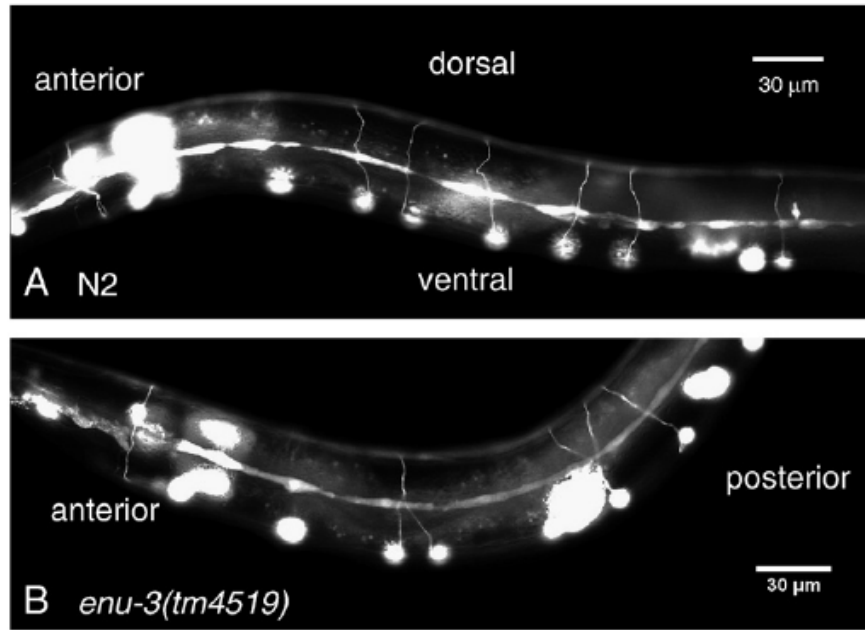
Figure 3.3: DA and DB axons of *enu-3* mutants have fasciculation defects and cross over each other.

A) The DA and DB motor neuron axons in N2 animals. B) DA and DB motor neuron axons in

enu-3(rq1) and *enu-3(tm4519)* animals have axon migration defects. These defects include axons

that migrate over each other and partial fasciculation defects. Seam cells illuminate the midline

of the animal.

Strain	DA3	DB4	DA4	DB5	DA5	DB6	DA6	DB7	DA7	% Affected	n
N2	2	4	0	0	1	0	0	0	0	4	100
enu-3(rq1)	19[c]	20[c]	4	7	13	3	3	1	2	35.6[c]	101
enu-3(tm4519)	23[c]	26[c]	4	10	9	15	5	1	1	41[c]	100
enu-3(rq1/tm4519)	25	25	4	9	9	9	2	0	4	35	106

Table 3.2: *enu-3(rq1)* and *enu-3(tm4519)* have increased axon migration defects relative to N2. The percentage of axons in N2, *enu-3(rq1)* and *enu-3(tm4519)* animals that have axon migration defects along with the percentage of affected animals (c indicates a *p* value of < 0.001 in a chi test). The fourth value represents the data obtained from the non-complementation study.

3.3   *enu-3(rq1)* and *enu-3(tm4519)* have mutations in the same gene

One genetic technique to determine if two mutations map to the same gene is an allelic complementation test. In an allelic complementation test, alleles of two homozygotes presumed to have mutations in the same gene are crossed together. Since *C. elegans* are diploid, the resulting F1 progeny will have a maternal and a paternally contributed copy of the gene. In theory, if the mutations lie in the same gene, the phenotypic defects of the F1 animals should be no worse than the strongest defective allele. However, if the mutations lie in different genes, the F1 animals should be wild-type and each animal has one "good" copy of each gene. Most genes are haplo-sufficient.

Based on the mapping data through microinjection, it is clear that H04D03.1 is the gene that is affected in *enu-3(rq1)*. To confirm the idea that *enu-3(rq1)* is an allele of H04D03.1, a known deletion allele of the same locus was used for the complementation study. The resulting F1 cross progeny had axon migration defects (Table 3.2), thus confirming the notion that the mutations in both alleles lie in the same gene. F1 cross progeny were confirmed by detection of a reporter transgene which was present in the males used for the cross (*syp-1*::dsRed2).

Complementation tests were also performed between *enu-3(rq1);unc-5(e53)* and *enu-3(tm4519);unc-5(53)*. Since the *unc-5(e53)* animals are too uncoordinated to mate, a different strategy was devised for the complementation test of the double mutant strains. In this case, *enu-3(rq1);him-5* males were crossed into *enu-3(rq1);unc-5(e53)* and the non-Dpy, non Unc males were crossed into *enu-3(tm4519);unc-5(e53)*. Non Dpy, non Unc F1 hemaphrodites were picked and the axon outgrowth defects of the Unc F2 generation were determined as shown in Table 3.1.

Again, the two alleles failed to complement each other indicating that both alleles possess mutations that are in the same gene.

One caveat of this experiment lies in the interpretation of genetic data. There are times when complementation tests produce an unexpected result due to intragenic complementation and non-allelic non-complementation. Intragenic complementation occurs when mutations of the same gene complement each other despite the fact that both alleles may not produce a functional protein. Non-allelic non-complementation occurs when two alleles that affect different genes do not complement and appear to be affecting the same gene. Since we know that *enu-3(tm4519)* has a deletion in H04D03.1, we can assume that *enu-3(rq1)* has a mutation in the same gene.

3.4   *enu-3* cDNA levels are altered in *enu-3(rq1)* relative to N2

Since the complementation studies cannot be conclusive due to the different types of complementation, the levels of *enu-3* mRNA were determined by performing semi-quantitative qPCR. mRNA, or messenger RNA, is generated from DNA in the nucleus and is modified and exported to the cytoplasm where it can be used as a template to generate its corresponding protein. Using various extraction techniques, total RNA can be isolated from whole animal lysates and can be converted to cDNA (complementary DNA) using the enzyme reverse transcriptase. The cDNA can then be used as a template by DNA polymerase and the amount of cDNA present for the gene of interest can be determined by comparing the intensity of the products of PCR amplification relative to a control (Figure 3.4). When the *enu-3* cDNA specific PCR products were made, two bands of the same sizes were present in both the experimental and control lanes. The larger band corresponds to an amplicon of 452 base pairs, which is a fragment

of unspliced *enu-3* cDNA. The smaller band corresponds to an amplicon of 348 base pairs, which is a fragment of spliced *enu-3*. It is quite evident that the intensity of the bands in N2 is stronger than those in *enu-3(rq1)*, suggesting that there is decreased amounts of the *enu-3* cDNA and subsequently mRNA.

A separate control experiment was performed using *ama-1*, a gene encoding the large subunit of RNA polymerase II. This transcript is expressed in extremely high levels during all stages of development and appeared to be the same intensity in both N2 and *rq1* (Figure 3.5). Two bands were observed which corresponded to the un-spliced and spliced versions of *ama-1*. In total, 4 bands were evident. It appears that the cDNA corresponding to the *ama-1* gene is present at approximately similar levels in both N2 and *enu-3(rq1)*, however the levels of the *enu-3* corresponding cDNA is less in *enu-3(rq1)* compared to N2. Thus, it can be concluded that there must be a mutation present in *enu-3(rq1)* that is affecting the levels of expression of *enu-3*. This mutation is most likely in the promoter region.
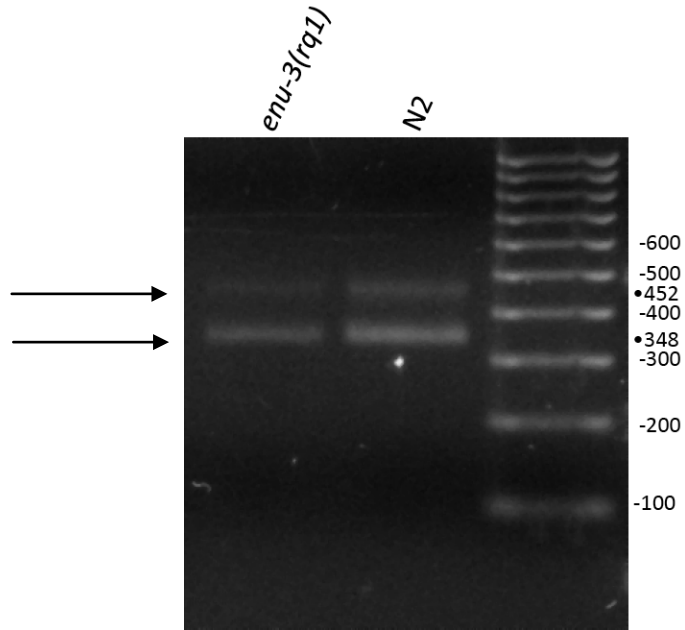
Figure 3.4: Gel electrophoresis of *enu-3* cDNA in *enu-3(rq1)* relative to N2.

Equal amounts of RNA of N2 and *enu-3(rq1)* worms were obtained and converted to cDNA

using reverse transcriptase. The resulting cDNA was used as a template for PCR amplification

using TaKaRa ExTaq and *enu-3* specific primers. Two products were obtained: one band at

348bp (corresponding to the spliced version of the *enu-3* gene product) and one band at 452bp

(corresponding to the un-spliced version of the *enu-3* gene product).
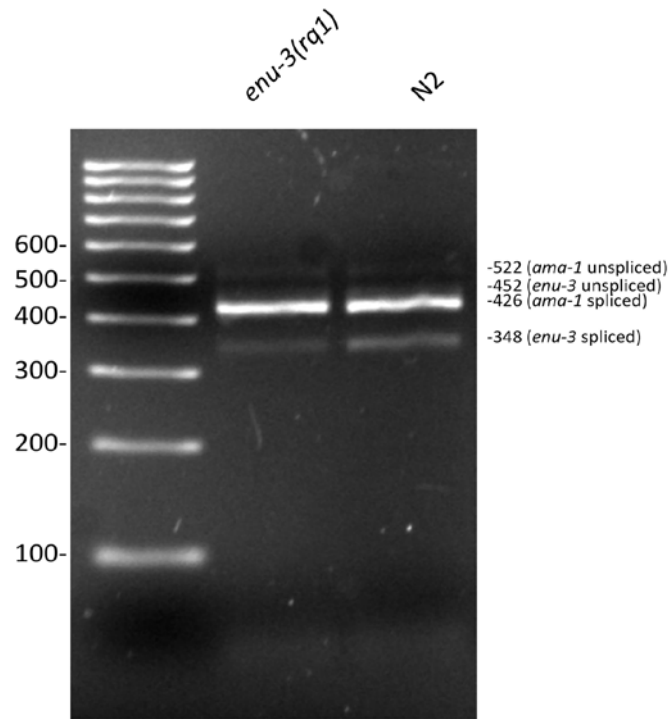
Figure 3.5: Gel electrophoresis of *enu-3* cDNA in *enu-3(rq1)* relative to N2.

Equal amounts of RNA of N2 and *enu-3(rq1)* worms were obtained and converted to cDNA

using reverse transcriptase. The resulting cDNA was used as a template for PCR amplification

using TaKaRa ExTaq and *enu-3* specific primers. Two products were obtained: one band at

348bp (corresponding to the spliced version of the *enu-3* gene product) and one band at 452bp

(corresponding to the un-spliced version of the *enu-3* gene product).

3.5   ENU-3 plays a role in short-range motor axon guidance in the UNC-6 pathway

In order to determine the effect of ENU-3 on motor neuron axon guidance, long range

and short range axon guidance defects were scored in single and double mutant animals. Axon

guidance defects were scored as described in the Materials and Methods using the *evIs82b*

transgene. *enu-3* mutants possess DA and DB motorneurons which reach the dorsal cord and

thus have no significant axon migration defects. In *unc-5(e53)*, almost all of the DA and DB

axons are unable to migrate to the dorsal side and instead exhibit a great deal of short and long

range migration defects (Table 3.3). However, in the double mutant background, *enu-3(tm4519)*

enhances *unc-5(e53)* slightly by converting some of the long range defects into short range

defects. In order to test the idea that ENU-3 is somehow functioning with UNC-5, a cross was

made to generate double mutants with a hypomorphic allele of *unc-5*, *unc-5(e152)*. *unc-5(e152)*

animals have a small percentage of short range defects (8%) and a large percentage of long range

defects (92%) (these numbers total 100%). However, when double mutants were made, the

percentage of short range defects increased significantly to 30% and long defects decreased to

70% accordingly. This suggests that *enu-3* is somehow involved in short-range guidance of the

motorneurons and also suggests that *enu-3* is working in the same pathway as *unc-5*.

To support the idea that *enu-3* is working in the UNC-6/Netrin pathway for axon

guidance, a cross was made between *unc-6(e78)*, a putative hypomorphic allele of *unc-6* (Table

3.3). A cross between *enu-3(tm4519)* and *unc-6(ev400)* was not examined as scoring the single

mutant, *unc-6(ev400),* was not possible due to the extreme complexity of axon guidance defects.

The *enu-3(tm4519);unc-6(ev400)* double mutant exhibited a slight enhancement of short range

guidance defects relative to the starting strain. To our surprise, *unc-40(e1430)* mutants were only

slightly enhanced with respect to axon guidance defects, supporting the notion that *enu-3* is

functioning with UNC-40, presumably in the UNC-6 pathway. UNC-40 is mainly involved in long range motor axon migrations and it appears that a mutation in ENU-3 enhances the short range migrations. A TGF-β related molecule, *unc-129*, has been shown to be responsible for long range guidance by breaking up UNC-5 homodimers and promoting the formation of UNC-5/UNC-40 heterodimers (MacNeil et al., 2009). *unc-129(ev554)* is a putative null mutant and has mainly long range guidance defects. Double mutants with *enu-3(tm4519)* did not enhance the axon guidance defects of *unc-129(ev554)*, suggesting that ENU-3 and UNC-129 either work in the same pathway or that they affect totally different processes.

It was previously reported that an axon guidance molecule, *clr-1*, functions in an UNC-6 independent pathway with UNC-40 (Chang et al., 2004). *clr-1* mutants do not have axon guidance defects alone, but when made as double mutants with *enu-3(tm4519)*, short range axon guidance defects were observed (Table 3.3). The result of this experiment has shown that *enu-3* plays a role in short range guidance and most likely functions in the same pathway as UNC-6.

Strain (all with *evIs82B*)	% Short Range	% Long Range	% DA Affected	% DB Affected	n
enu-3(tm4519)	0	0	0	0	<100
enu-3(rq1)	0	0	0	0	<100
unc-5(e53)	42	58	92	94	104
enu-3(tm4519);unc-5(e53)	48	52	92	93	137
unc-5(e152)	8	92	85	80	103
enu-3(tm4519);unc-5(e152)	30^c	70^a	80	85	109
unc-6(e78)	2	98	65	87	102
enu-3(tm4519);unc-6(e78)	8^a	92^a	79	91	95
unc-40(e1430)	8	92	26	32	114
unc-40(e1430);enu-3(tm4519)	10	90	26	28	102
unc-129(ev554)	5	95	38	54	101
enu-3(tm4519);unc-129(ev554)	4	96	39	55	100
clr-1(e1745)	0	0	0	0	120
clr-1(e1745);enu-3(tm4519)	100	0	2	6	100

Table 3.3: *enu-3* plays a role in short-range guidance of the DA and DB motoraxons.
Strains are indicated in the first column. The percentage of animals with defects in
short-range (before the seam cell) or long-range (after the seam cell) migrations is
indicated (scored as described in MacNeil et al., 2009). The percentage of animals with
migration defects in the DAs and DBs is shown. n is the number of animals scored.

[a] Means a *p* value of less than 0.01.

[b] Means a *p* value of less than 0.001.

[c] Indicates a *p* value on a chi test of less than 0.0001.

3.6 *enu-3* **mutants can be rescued by the H04D03.1 gene product**

Previously, mapping by others has shown that H04D03.1 is the gene affected in *enu-3(rq1)* (Sybingco, 2008). Microinjection of a cloned copy of H04D03.1 has been shown to rescue the motor axon outgrowth defects of *enu-3(rq1);unc-5(e53)* significantly as shown in Table 3.4. This same cloned copy was shown to rescue the double mutant of *enu-3(tm4519);unc-5(e53)*. The rescue was complete, and in both rescued lines, rescue of the outgrowth defects of *enu-3(rq1);unc-5(e53)* were even better than the *unc-5(e53)* mutant alone. The number of copies within the extrachromosomal array was not determined. As a control for this experiment, *enu-3p::gfp* was crossed into the double mutants and assessed for rescue. As expected, the transcriptional fusion did not rescue the defects as the transgene lacks a functional copy of *enu-3*. However, a translational GFP fusion construct was also generated and partial rescue of the outgrowth defects of the double mutant was observed. Full rescue was not attained by the transgene, most likely due to the presence of the GFP tag at the C-terminus of the ENU-3 protein.

As mentioned previously, *enu-3* single mutants have a high penetrance of axon migration defects (approximately 36% for *rq1* and 41% for *tm4519,* Table 3.2). The same extrachromosomal array that rescued the motor neuron axon outgrowth defects was able to rescue the axon migration defects of both alleles of *enu-3*(Table 3.5). The transcriptional reporter in contrast, did not rescue the defects (Table 3.5). Interestingly, the extrachromosomal array containing the translational fusion was able to rescue the defects back to wild-type level. This extrachromosomal array however did not fully rescue the axon outgrowth defects of the double mutant *enu-3(tm4519);unc-5(e53)*.

Strain (all containing evIs82B)	DB4	DA4	DB5	DA5	DB6	%	n
unc-5(e53)	6	2	10	2	6	27	100
enu-3(rq1);unc-5(e53)	14	1	19	1	13	50	100
enu-3(rq1);unc-5(e53)[enu-3(+)]	2[b]	6	4[b]	2	0	20[b]	100
enu-3(tm4519);unc-5(e53)	30	18	32	4	32	40	100
enu-3(tm4519);unc-5(e53)[enu-3(+)]	4[b]	2	6[b]	0	2	16[b]	100
enu-3(tm4519);unc-5(e53)[enu-3p::gfp]	31	17	30	4	28	40	84
enu-3(tm4519);unc-5(e53)[enu-3(+)::gfp]	10[b]	5	15[b]	1	10	29[a]	100

Table 3.4: Expression of H04D03.1 rescues axon outgrowth defects of *enu-3;unc*-5 mutants. The strains containing the transgenes indicated in the first column were scored for motor axon outgrowth defects. The percentage of defects in the indicated motor neuron axon is shown in each case. The percentage of worms that display the defect at least in one of the motor neurons is given under '%' column. Each transgene contains *myo-2::yfp* as a co-transformation marker. The number of animals scored is shown in n.

[a] Means a *p* value of less than 0.01.

[b] Means a *p* value of less than 0.001

Strains (all containing *evIs82B)*	% of affected animals	n
N2	4	100
enu-3(rq1)	36[c]	101
enu-3(rq1)[enu-3(+)]	7[c]	107
enu-3(tm4519)	41[c]	100
enu-3(tm4519)[enu-3(+)]	10[c]	100
enu-3(tm4519)[enu-3p::gfp]	38[c]	50
enu-3(tm4519)[enu-3(+)::gfp]	4[c]	79
enu-3(tm4519)[unc-129p::enu-3(+)::gfp]	8[c]	100

Table 3.5: Expression of H04D03.1 rescues axon migration defects of *enu-3* mutants

The strains containing the transgenes indicated in the first column were scored for motor axon migration defects. The percentage of defects in the indicated motor neuron axon is shown in each case. The percentage of worms that display the defect at least in one of the motor neurons is given under '%' column. Each transgene contains *myo-2::yfp* as a co-transformation marker. The number of animals scored is shown in n.

[a] Means a *p* value of less than 0.01.

[c] Means a *p* value of less than 0.001.

3.7   ENU-3 functions cell autonomously in the DA and DB motorneurons

In order to test the idea that ENU-3 functions cell autonomously in the DA and DB motorneurons, a construct was generated where the *unc-129* promoter was used to "drive" transcription of a translational fusion of *enu-3::gfp*. This promoter is known to selectively express in the DA and DB cells. If all of the machinery required for proper function and signalling of *enu-3* is found within the cell, then this construct would rescue the defects of the mutant and thus ENU-3 functions cell autonomously. If no rescue was observed, it indicates that *enu-3* requires some other receptors or signalling partners that lie outside of the cell for proper functioning to occur.

This transgene and the resulting extrachromosomal array were able to rescue the defects of the *enu-3(tm4519)* mutants, where the percentage of affected animals was reduced from 41% to 8% (Table 3.5). Based on these results, it can be concluded that ENU-3 does indeed function cell autonomously in the DA and DB motor neurons.

3.8   ENU-3 is expressed in the nervous system

Transcriptional and translational reporters were generated as described in Chapter 2. In all lines generated, a single cell known as the PVT showed expression of GFP. The PVT is an interneuron found in the pre-anal ganglion of the worm. The transcriptional fusion revealed expression throughout the nervous system and in some lines was shown to express weakly in individual dorsal and ventral muscle cells (Figure 3.5).

The most definitive expression pattern is shown in Figure 3.6 where a *him-5(e1420);dpy-20(e1282)* animal was injected with the translational fusion and a wild-type copy of *dpy-20* was used as a co-injection marker (Figure 3.5). The expression pattern resembles a weak pan-neuronal reporter, as expression is widespread throughout the nervous system of the animal. Expression was noted chiefly in the ventral and the motorneurons which lie on the ventral nerve cord. Weak expression can be observed in various commissures and axons which have not been identified yet. However, it can be concluded that expression of ENU-3::GFP is within the DA and DB motorneurons, as expected based on our initial screen.
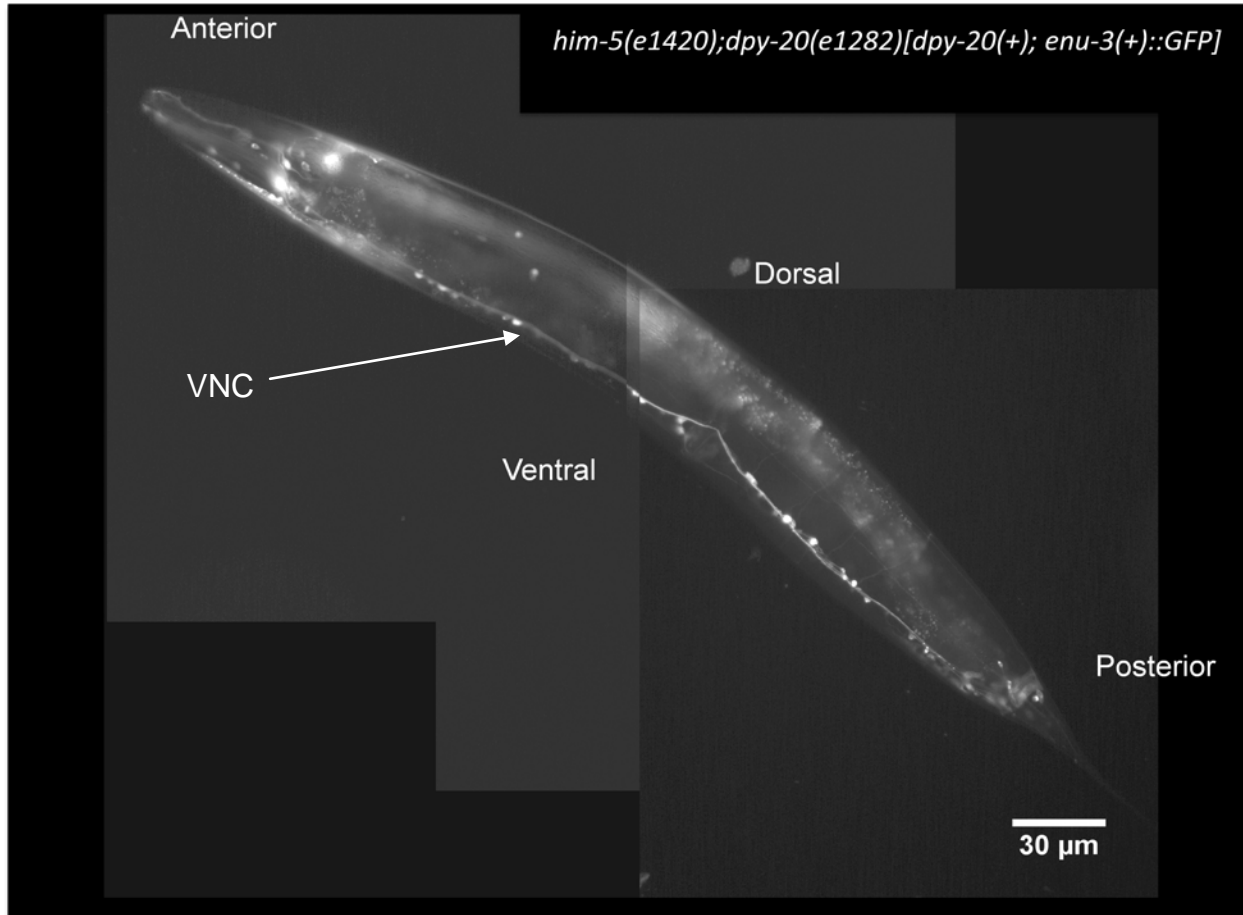
Figure 3.6: The expression pattern of ENU-3::GFP.

A composite picture of a *him-5(e1420);dpy-20(e1282)* L4 animal expressing ENU-3::GFP with

dpy-20 as a co-injection marker. The picture was taken at 400x magnification.

3.9　　　　　Predicted Structure of ENU-3

H04D03.1/*enu-3* is comprised of 3 exons which are predicted to encode for a protein 204 amino acids in size with a molecular weight of 22,702 kDa. The corresponding protein, ENU-3, has the Wormbase protein designation WP:CE16165 and is a member of the homology group LSE0872. Structural analysis suggests that ENU-3 possesses a signal peptide cleavage site after amino acid residue 23, resulting in removal of residues 1-23. Other key features of ENU-3 are that it possesses a predicted transmembrane domain from residues 108-128 and a coiled-coil region from residues 144-165. Based on these domains, it can be hypothesized that ENU-3 is likely to be a single-pass type I transmembrane protein.

Homology searches using the ENU-3 protein sequence yielded no significant results, suggesting that a homologue of ENU-3 in other organisms may possibly exist at the structural level as opposed to amino acid sequence homology. ENU-3 appears to possess homology to proteins in other worm species: *C. briggsae* possesses a homologous protein of 432 residues called CB18306, *C. ramanei* possesses a homologous protein of 462 residues called CRE04841 and *C. brenneri* possesses a homologues protein of 462 residues called CN12308. ENU-3 also appears to be weakly homologous to two uncharacterized human protein fragments that contain potential tropomyosin domains (ENSP00000389730 and ENSP00000413808). Tropomyosin has been shown to associate with actin, troponin and tropomodulin. These associations have been shown to play a major role in regulation of the cytoskeleton and in muscle contraction (Gunning et al., 2008).
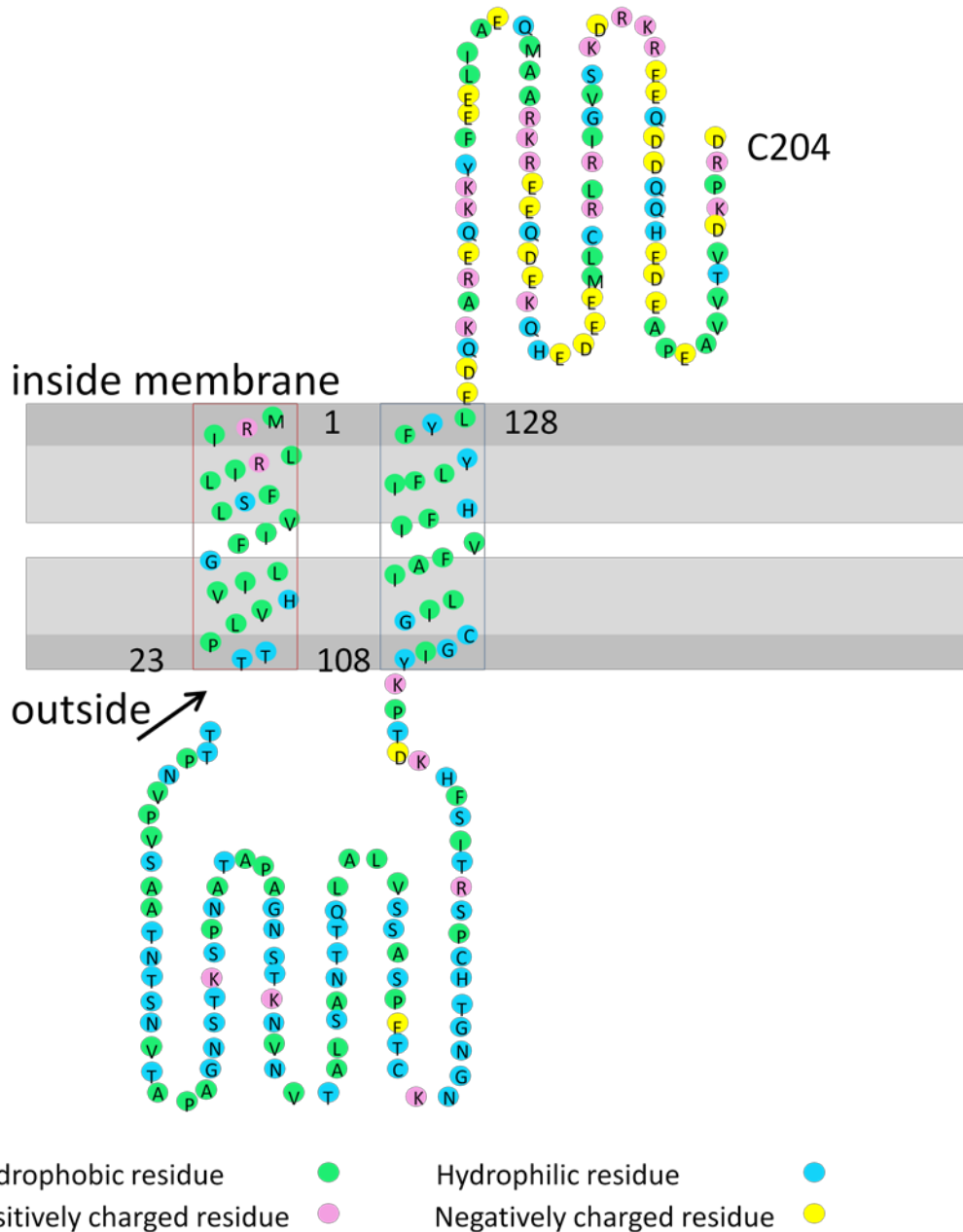
Figure 3.7: Predicted Structure of ENU-3.

ENU-3 appears to be a predicted single-pass transmembrane protein of 204 amino acid residues.

ENU-3 possesses a signal peptide which is cleaved after residue 23 and a coiled-coil region from

residues 144-165. The N-terminus begins at amino acid 24 and the C-terminus is at amino acid

204.

3.10   Paralogs of ENU-3

BLAST searches using the ENU-3 protein sequence indicate that *C. elegans* contains four

other proteins that are paralogous to ENU-3, all novel proteins of unknown function. Protein

sequence alignment of ENU-3 to its paralogs has revealed that most of the paralogs contain

almost all of the ENU-3 sequence but are much larger and possess 2-3 extra exons. ENU-3 is

predicted to be 204 amino acids while W03G9.3 is 462 amino acids, W05F2.2 is 457 amino

acids, C38D3.1a is 462 amino acids and Y37D8a.12a is 458 amino acids. However, at the amino

terminus, all of the paralogs of ENU-3 possess greater than 90% identity to ENU-3. The

homology is shown in Figure 3.8. Comparison of the promoters of the paralogs yielded no

information with respect to common elements.

```
C38D4.1     MRILRILFSLVIFGLIVHVLPTTTTPNVPVSAATNTSNVTAPAGNSAKSPNATAPAGNPT 60
Y37D8A.12   MRILCILFSLVIFGLIVHVLPTTTTPNVPVSAATNTSNVTAPT----KSPNATAPAGNST 56
W03G9.3     MRILRILFSLVIFGLIVHVLPTTTTPNVPVSAATNTSNVTAPAGNSTKSPNATAPAGNST 60
W05F2.2     MRILRILFSLVIFGLIVHVLPTTTTPNVPVSAATNTSNVTAPAGNSTKSPNATAPAGNST 60
H04D03.1    MRILRILFSLVIFGLIVHVLPTTTTPNVPVSAATNTSNVTAPAGNSTKSPNATAPAGNST 60
            **** ************************************:    ***********.*

C38D4.1     KNVNVTAPAANTTQLALVSSASPQTCKNGNGTHCPSCAYTINVHKDTPKYIGYGILIAFV 120
Y37D8A.12   KNVNVTAPAANTTQLALVSSASPQTCKNGNGTHCPSCAYMINVHKDTPKYIGYGILIAFV 116
W03G9.3     KNVNVTAPAANTTQLALVSSASPQTCKNGNGTHCPSCAYTINVHKDTPKYIGYGILIAFV 120
W05F2.2     KNVNVTAPAANTTQLALVSSASPQTCKNGNGTHCPSCAYTINVHKDTPKYIGYGILIAFV 120
H04D03.1    KNVNVTALSANTTQLALVSSASPETCKNGNGTHCP--SRTISFHKDTPKYIGCGILIAFV 118
            ******* : **************:**********   : *..********* *******

C38D4.1     IFHIFLYFYLEDQKAREQKKYFEELIAEQMAARKREEQDDQQHEDEEKERRERLAYGIAA 180
Y37D8A.12   IFHIFLYFYLEDQKAREQKKYFEELIAEQMAARKREEQDDQQHEDEEKERRERLAYGIAA 176
W03G9.3     IFHIFLYFYLEDQKAREQKKYFEELIAEQMAARKREEQDDQQHEDEEKERRERLAYGIAA 180
W05F2.2     IFHIFLYFYLEDQKAREQKKYFEELIAEQMAARKREEQDDQQHEDEEEDERR----GTPR 176
H04D03.1    IFHIFLYFYLEDQKAREQKKYFEELIAEQMAARKREEQDEKQHEDEE------------- 165
            *******************************************::******

C38D4.1     NPYVVAESKTPNGNVTKVMEKRRSAVAPPITPALGAGSTNGPYESRTKTAQKEEAMSCHL 240
Y37D8A.12   NPYVVAESKTPNGNVTKVMEKRRSAVAPPITPALGAGSTNGPYESRTKTAQKEEAMSCHL 236
W03G9.3     NPYVVAESKTPNGNVTKVMEKRRSAVAPPITPALGAGSTNGPYESRTKTAQKEEAMSCHL 240
W05F2.2     -AYVVAESKTSNGNVTKVMEKRRSAVAPPITPALGAGSINGPYESRTKTAQKEEAISCHL 235
H04D03.1    --------------------------------------------------------MLCRL 170
                                                             : *:*

C38D4.1     QVIADNWGRGKELISLINDLDLPAPLVTTEEKARYALELVQHHVEKMTEQKVFLHGYLDD 300
Y37D8A.12   QVIADNWGRGKELISLINDLDLPAPLVTTEEKARYALELVQHHVEKMTEQKVFLHGYLDD 296
W03G9.3     QVIADNWGRGKELISLINDLDLPAPLVTTEEKARYALELVQHHVEKMTEQKVFLHGYLDG 300
W05F2.2     QVIADNWGRGKELISLINDLDLPAPLVTTEEKARYALELVQHHVEKMTEQKVFLHGYLDD 295
H04D03.1    RIGVS------------------------------------------------------- 175
            :: ..

C38D4.1     GPPFVCSSETLAKEIFSDARLELKLELTSPVHMKMDVFSVKLEPQQKTVLPEPTKETPKT 360
Y37D8A.12   GPPFVCSSETLEKEIFSDARLELKLELTSPVHMKMDVFSVKLEPQQKTVLPEPTKETPKT 356
W03G9.3     GPPFVCSSETLAKEIFSDTRLELKLELTSPVHMKMDVFSVKLEPQQKTVLPEPTKETPKT 360
W05F2.2     GPPFVCSSDTLAKEIFSDARLELKLELTSPVHMKMDVFSVKLEPQQKTVLPEPTKETPKT 355
H04D03.1    ------------------------------------------------------------

C38D4.1     DALLTPGSHIKGRSMAAESSKRKAPKVSTDLTNLVPLLQQAQMLPVTEKATKEKLQTPKQ 420
Y37D8A.12   DALLTPGSHIKGRSMAAESSKRKAPKLSTDLTNLVPLLQQAQMLPVTEKATKEKLQTPKQ 416
W03G9.3     DALLTPRSHIKGRSMAAESSKRKAPKLSTDLTNLVPLLQQAQMLPVTEKATKEKLQTPKQ 420
W05F2.2     DALLTPGSHIKGRSMAAESSKRKAPKLSTDLTNLVPLLHQAQMLPVTEKATKEKLQTPKQ 415
H04D03.1    ----------KDR-------KR--------------------------------------- 180
                       *.*       **

C38D4.1     SPMPGTPENTSLPPSLIKKKKKEWTSEQAAPEAVVTVDKPRD 462
Y37D8A.12   SPMPGTPENTSLPPSLIKKKKKESTSEQAAPEAVVTVDKPHD 458
W03G9.3     SPMPGTPENTSLPPSLIKKKKKESTSEQAAPEAVVTVDKPHD 462
W05F2.2     SPMPGTPENTTLPPSLIKKKKKESTSEQAAPEAVVTVDKPHD 457
H04D03.1    ------------------EEQDDQQHEDEAPEAVVTVDKPRD 204
                      :::.: :      ***********:*
```

Figure 3.8: Amino acid alignment of H04D03.1 to its protein paralogs.

H04D03.1 appears to be a smaller member of 5 extremely homologous proteins in *C. elegans*.

3.11   Knockdown of H04D03.1 by RNA Inhibition

In order to show independent proof that H04D03.1 is the correct gene that is affected in *enu-3(rq1)*, RNAi knockdown of the H04D03.1 gene transcript was performed in N2 and in *unc-5(e53)* worms. Animals were scored for the presence of the axon migration defects, as observed in *enu-3(rq1)* and *enu-3(tm4519)*, and axon outgrowth defects, as observed in *enu-3(rq1);unc-5(e53)* and *enu-3(tm4519);unc-5(e53)*. An RNAi vector that possessed no gene insert was used as a control in all cases.

The treatment of the empty vector did cause slight axon migration and axon outgrowth defects, however these defects were not significant. As expected, the H04D03.1 RNAi clone from the Ahringer library caused both axon migration and axon outgrowth defects. The defects that were observed occurred predominantly in DA3/DB4 for axon migration and DB4/DB5/DB6 for outgrowth as shown in Table 3.6 and Table 3.7. These results also agree with the double mutant data as described in this work and this is somewhat surprising as RNA inhibition frequently does not work in the neurons.

unc-5(e53)	DB4	DA4	DB5	DA5	DB6	%	n
No Treatment	6	2	10	2	6	27	100
Empty Vector	6	2	12	3	6	29	107
H04D03.1 RNAi clone	12[a]	3	20[a]	4	10	43[a]	102

Table 3.6: RNAi of H04D03.1 on *unc-5(e53)* mutants enhances outgrowth defects

The strains containing the transgenes indicated in the first column were scored for motor axon

outgrowth defects. The percentage of defects in the indicated motor neuron axon is shown in

each case. The percentage of worms that display the defect at least in one of the motor neurons is

given under '%' column.

[a] Means a *p* value of less than 0.001.

N2	DA3	DB4	DA4	DB5	DA5	DB6	DA6	%	n
No Treatment	3	3	0	1	1	0	0	4	100
Empty Vector	3	4	1	1	1	1	0	6	102
H04D03.1 RNAi clone	13[a]	14[a]	1	3	3	2	3	20[a]	100

Table 3.7: RNAi of H04D03.1 on wildtype (N2) worms causes axon migration defects

The strains containing the transgenes indicated in the first column were scored for motor axon migration defects. The percentage of defects in the indicated motor neuron axon is shown in each case. The percentage of worms that display the defect at least in one of the motor neurons is given under '%' column.

[a] Means a p value of less than 0.001.

3.12   _enu-3_ is not likely to play a major role in the VD/DD motorneurons

Although expression of _enu-3_ is likely to be in the VD and DD motorneurons based on the expression experiments, _enu-3_ is unlikely to play a major role regarding migration of the commissures. The _unc-47_::GFP reporter was used to examine the VD and DD motorneurons and there was no difference between the marker line and _enu-3(tm4519)_ mutants (47 animals scored). Fasciculation and migration defects were common among the animals scored, but the marker itself causes a great deal of migration defects in wildtype (Peter Roy, personal communication). Both N2 and _enu-3(tm4519)_ mutants with the transgene possessed approximately an average of 36% axon migration defects in each animal.

3.13   _enu-3_ is involved in ventral guidance of the AVM and PVM neurons

The guidance of the cell body and the axons in the mechanosensory neurons is dependent on UNC-6 working through UNC-40. UNC-5 is not involved, so we expected that ENU-3 would play a role in dorsally directed migrations of the motor neuron axons but none in the migrations of the mechanosenosory neurons or their axons. However, since the results have shown that _enu-3_ may be functioning somehow with the UNC-6 pathway, we tested to determine whether the protein affects guidance of the motor neurons. Guidance of the AVM and PVM neurons was analyzed using a marker specific for the six mechanosensory neurons (_mec7p::gfp_). In _unc-40(e1430)_ mutants, the PVM cell body is frequently misplaced and fails to migrate from its initial anterior position to a more posterior location (Chan et al., 1996). The PVM in these mutants can be often found close by the AVM cell body or adjacent to one of the ALM cell bodies. In these mutants, the AVM and PVM axons have been observed to sometimes migrate in

an anterior direction instead of the normal ventral direction. In *unc-6(ev400)* mutants, anterior axon migration has been observed but the translocation defects of the soma seen in *unc-40* mutants are absent, suggesting that UNC-40 must play a role in the posterior migration of the PVM cell body and the migration in the ventral direction of its axon.

enu-3 mutants do not have any obvious ventral guidance defects in the mechanosensory cell bodies or placement of the axons as single mutants. However, in *unc-40(e1430);enu-3(tm4519)*, there were significant enhancements of the AVM and PVM cell body positioning and axon guidance defects, as shown in Table 3.8. In the double mutants with *unc-40(e1430)*, the PVM cell body was almost always misplaced in the anterior portion of the animal. The axon emanating from the PVM often migrated in an anterior direction and then ventrally. The PVM axons, when not mislocated, sometimes tended to twist and make ribbon like structures. In rare cases, the PVM appeared to be multipolar and project axons ventrally, dorsally, anteriorly and posteriorly. Defective AVM axons that were observed almost always migrated anteriorly, joining up with one of the ALM axons and migrating towards the head. Interestingly, *enu-3(tm4519)* did not enhance the defects of *unc-6(ev400)*. Doubles were confirmed by the reduced brood size and appearance of extreme uncoordination of animals on the plate. Based on these results, it can be concluded that mutations in *enu-3* enhance *unc-40* mutants but do not enhance *unc-6* mutants, suggesting that *enu-3* functions in an UNC-6 dependent, UNC-40 independent pathway.

In order to prove that *enu-3* lies in the UNC-6 pathway for ventral guidance, *enu-3* mutants were crossed with *slt-1* mutants (Table 3.8). As mentioned in the introduction, there are two pathways known for ventral guidance of the AVM and PVM neurons, the UNC-6 pathway and the SLT-1 pathway. It has been shown that there is crosstalk between these two pathways, where SAX-3 binds to UNC-40 to prevent ventral guidance signalling altogether in the absence

of SLT-1 or EVA-1 (Fujisawa et al., 2007). However, in the absence of UNC-6 or its receptor UNC-40, the SLT-1 pathway compensates for the loss and there is increased signalling activity. *slt-1(eh15)* is a putative null allele of *slt-1* and acts chiefly in the AVM, where 40% of the AVM cells are affected (Hao et al., 2001). It plays a much more minor role in the PVM for reasons that are not yet understood. The double mutant with *enu-3(tm4519)* enhanced the ventral guidance of the PVM and AVM axons defects of *slt-1(eh15)* significantly, thus confirming the notion that ENU-3 is functioning in a pathway parallel to the SLT-1 pathway and most likely in the UNC-6/UNC-40 pathway.

Strain (all with *mec7p::GFP*)	% AVM Defective	% PVM Defective	n
enu-3(tm4519)	0	0	<100
unc-40(e1430)	19	27	251
unc-40(e1430);enu-3(tm4519)	39[a]	50[a]	139
unc-6(ev400)	36	46	200
enu-3(tm4519);unc-6(ev400)	37	47	94
slt-1(eh15)	40	3	109
enu-3(tm4519);slt-1(eh15)	53[b]	7[a]	120

Table 3.8: *enu-3* enhances the ventral guidance defects of *unc-40* and *slt-1* but not *unc-6*. The strains containing the transgenes indicated in the first column were scored for AVM and PVM defectiveness. Defectiveness is defined in the materials and methods and includes misplacement of either the cell body or the axon.

[a] Means a *p* value of less than 0.01.

[b] Means a *p* value of less than 0.001.

3.14   *enu-3* is involved in distal tip cell guidance

The distal tip cells are located at the leading edge of the gonad and they lead the gonad as it migrates along the ventral side of the animal away from the vulva, turns and migrates in a dorsal direction and then reflexes back towards the vulva on the dorsal side. These ventral to dorsal migration appears to rely on the presence of UNC-5 (Su et al., 2000: Killeen et al., 2002). In wild-type animals and in *enu-3(tm4519)* animals, distal tip cell (DTC) defects are relatively rare. However, *unc-40(e1430)* mutants have mild DTC defects and are significantly enhanced when both UNC-40 and ENU-3 are mutated/absent. Double mutants were constructed using *enu-3(tm4519)* and UNC-6 pathway mutants. The distal tip cell defects of either *unc-5(e53)* or *unc-6(ev400)* were not enhanced by a mutation in ENU-3, suggesting that *enu-3* is functioning in the same pathway as UNC-5 and UNC-6 but parallel to UNC-40 for DTC guidance.

Strain	% Anterior Defective	% Posterior Defective	n
N2	0	1	97
enu-3(tm4519)	0	2	152
unc-40(e1430)	3	26	100
unc-40(e1430);enu-3(tm4519)	37[a]	48[a]	193
unc-6(ev400)	47	65	92
enu-3(tm4519);unc-6(ev400)	47	62	126
unc-5(e53)	29	60	100
enu-3(tm4519);unc-5(e53)	31	60	101

Table 3.9: *enu-3* enhances the distal tip cell defects of *unc-40(e1430)*.

Animals were scored under 400x magnification and gonads were considered defective if the gonad reflexed back towards the vulva during the first turn, resulting in a ventral clear patch.

[a] Means a *p* value of less than 0.0001.

Chapter 4.   Discussion

The only known pathway to control dorsal guidance of the DA and DB motorneurons is the UNC-6/Netrin pathway. However, in the absence of the ligand UNC-6 or its key receptor for axon outgrowth, UNC-5, axon outgrowth is only moderately reduced, indicating the presence of an alternative pathway controlling axon outgrowth (Table 3.1). The experiments that were performed in this study were directed towards finding and characterizing a gene that functions to control axon outgrowth of the DA and DB motorneurons. The original genetic enhancer screen was conducted in an *unc-5(e53)* background, seeking double mutants that possessed enhanced motor axon outgrowth defects. The results of the screen have generated 5 putative candidate mutations, numbered *rq1* to *rq5*. This current study has focused on characterizing the *rq1* allele, originally isolated by Sybingco (2008).

4.1   ENU-3 is involved in axon outgrowth and guidance of the DA/DB motorneurons

The *enu-3(rq1)* mutation was shown to significantly enhance the axon outgrowth defects of putative null alleles of both *unc-5* and *unc-6*, thus indicating that *enu-3* most likely functions parallel to the UNC-6 pathway (Table 3.1). However, enhancement does not always indicate parallel function. If ENU-3 functioned upstream of the UNC-6 pathway, enhancement would be observed in the double mutants as the absence of UNC-6 causes more significant defects than absence of ENU-3. This idea is unlikely as UNC-6 signalling occurs early during development to control many different processes. The structural predictions of ENU-3 indicate that it is a trans-membrane protein and would most likely work parallel to UNC-5 and UNC-40 during axon

71

outgrowth. ENU-3 was found to be expressed embryonically as well as in all larval stages and adults.

The data that has been generated regarding motor axon guidance show that ENU-3 is involved in short range guidance of the DA and DB motorneurons. It has long been known that UNC-5 is responsible for the repulsion mechanism involved in UNC-6 signalling (Hedgecock et al. 1990; Leung-Hagesteijn et al. 1992). UNC-5 can exist as homodimers or heterodimers with UNC-40. UNC-5 homodimers and similarly UNC-5/UNC-40 heterodimers are repulsed by the source of UNC-6 and thus guide the axon dorsally. The true purpose of UNC-40 with respect to axon guidance is less clear although in *Drosophila* UNC-40/Frazzled is required for long range migrations (Keleman et al., 2001). Macneil et al. (2009) showed that another molecule, UNC-129, plays a role in regulating the balance of UNC-5/UNC-40 heterodimers and UNC-5 homodimers. MacNeil et al. (2009) has shown that UNC-40 is responsible for long range guidance of the motorneurons just as in *Drosophila*. UNC-129 is able to dissociate UNC-5 homodimers and allow for UNC-5/UNC-40 heterodimer formation. The creation of these heterodimers allows the motorneurons to achieve the correct trajectory and innervate the intended target. Thus, the presence of these heterodimers seems to be the most favourable option for axon guidance to the dorsal side. If this is so, possibly UNC-5 homodimers are not required at all.

In order to test the idea that ENU-3 is involved in the guidance of short range motor axons, double mutants with *clr-1*, a receptor tyrosine kinase that has been shown to function in an UNC-6 independent pathway with UNC-40, were constructed (Chang et al., 2004). Interestingly, the absence of ENU-3 was able to generate short range defects in the double mutants, while both single mutants have no axon guidance defects. One possibility is that ENU-3

72

is functioning somehow similarly to UNC-129 in the sense that it somehow shifting the balance between UNC-5 and UNC-40 receptor combinations. For instance it is possible that ENU-3 prevents UNC-40 homodimer formation in favour of UNC-40/UNC-5 heterodimers.

The absence of ENU-3 did not enhance any of the UNC-6 pathway mutants for motor axon guidance, suggesting that it lies within this pathway for axon guidance. This concept seems strange since the screen was directed towards identifying axon guidance molecules that function parallel to this pathway for axon outgrowth. It may be that ENU-3 does not play a role in axon guidance at all, however *enu-3* mutants enhance hypomorphs of *unc-6* and *unc-5* that are both involved in motor neuron guidance, so ENU-3 appears to play some role in motor axon guidance.

ENU-3 could be functioning opposite to UNC-129 in order to facilitate axon outgrowth of the DA and DB motorneurons. During axon outgrowth, at least UNC-5/UNC-40 heterodimers are required to be present on the growth cone of the developing axon. Since UNC-40 is attracted to UNC-6, if the axon possesses UNC-40 homodimers, the UNC-40 homodimers may presumably counter the repulsion of UNC-5 and thus result in failure of the axon to leave the cell body. Thus, based on this reasoning, there must be something that is preventing UNC-40 homodimer formation during axon outgrowth. ENU-3 most likely could make heterodimers with UNC-40, preventing UNC-40 from binding with UNC-5 and thus allowing for proper axon outgrowth. Alternatively, if UNC-5/UNC-40 heterodimers are preferred for axon outgrowth, UNC-129 could be breaking up UNC-5 homodimers and ENU-3 could be breaking up UNC-40 homodimers, thus promoting formation of UNC-5/UNC-40 heterodimers.

A surprising result was found when the *unc-40(e1430);unc-5(53)* double mutant was analyzed for motor axon outgrowth defects (Table 3.1). This mutant had very few axon

outgrowth defects, suggesting that the mutation in *unc-40(e1430)* suppressed the axon outgrowth

defects. Therefore the axons can grow out without input from either UNC-5 or UNC-40. This

suppression suggests that UNC-40 is somehow involved in opposing axon outgrowth out of the

ventral cord, which is quite contradictory to the current understanding of UNC-40 but consistent

with the effect of UNC-6 on UNC-40 (which is attraction). Interestingly, the triple mutant *unc-*

40(e1430);enu-3(tm4519);unc-5(e53) had more defects than *unc-40(e1430);unc-5(e53)* but less

than *enu-3(tm4519);unc-5(e53)*. This slight enhancement relative to the double mutant between

unc-5 and *unc-40* suggests that ENU-3 possesses some sort of axon outgrowth activity that is

independent of UNC-5 and UNC-40.

There is currently one known pathway for axon outgrowth of the DA and DB

motorneurons. This pathway involves UNC-6 signalling to UNC-5 homodimers or UNC-5/UNC-

40 heterodimers (Figure 4.1). The chemorepulsion elicited by UNC-5 thus guides the growth

cone of the developing axon towards the dorsal side of the animal. The second pathway inferred

from our data may involve UNC-6 signalling to UNC-40 heterodimers with ENU-3 and possibly

other proteins. The suppression of motor axon outgrowth defects of *unc-5(e53)* by *unc-*

40(e1430) could suggest that UNC-40 is acting either upstream or parallel to UNC-5 to control

axon outgrowth. Since it is very unlikely that UNC-40 is acting upstream of UNC-5, it can be

thus concluded that it is functioning parallel to control this mechanism. ENU-3 is a relatively

small protein and could form a complex to bind to UNC-40 to control axon outgrowth.

Although this idea seems promising, the other mechanisms controlling axon outgrowth in the DA

and DBs remain unknown. The double mutant with *unc-5* still had axons which had normal axon

outgrowth, indicating that there are still other proteins involved in this process. These other

proteins are likely to play a much more significant role in outgrowth over the UNC-6/Netrin

pathway or ENU-3. Potential *c*lues towards solving this problem lie with respect to ENU-3's

protein paralogs. In *C. elegans*, ENU-3 possesses 5 paralogs, where 4 are highly homologous to

the sequence of *enu-3*. Recent RNAi data performed by Suzan El-Rass (member of the Killeen

group) has shown that RNAi knockdown of the orthologs in an *unc-5(e53)* background has

increased levels of axon outgrowth defects relative to the empty vector treatment. The increased

levels of defects are significant and resemble the axon outgrowth defects of the *enu-*

3(tm4519);unc-5(e53) mutant. Interestingly, knockdown of some of the paralogues affects

different axons than those altered by *enu-3;unc-5(e53)*. However, a criticism of this experiment

is that the RNAi vectors being used may actually have multiple targets and that the RNAi clones

may actually be silencing H04D03.1. The RNAi data is thus inconclusive until knockout or null

alleles are made available. Fortunately, two mutants are now available – W03G9.3 (*tm5189)* and

C38D4.1(*tm5039)* so this can be tested.
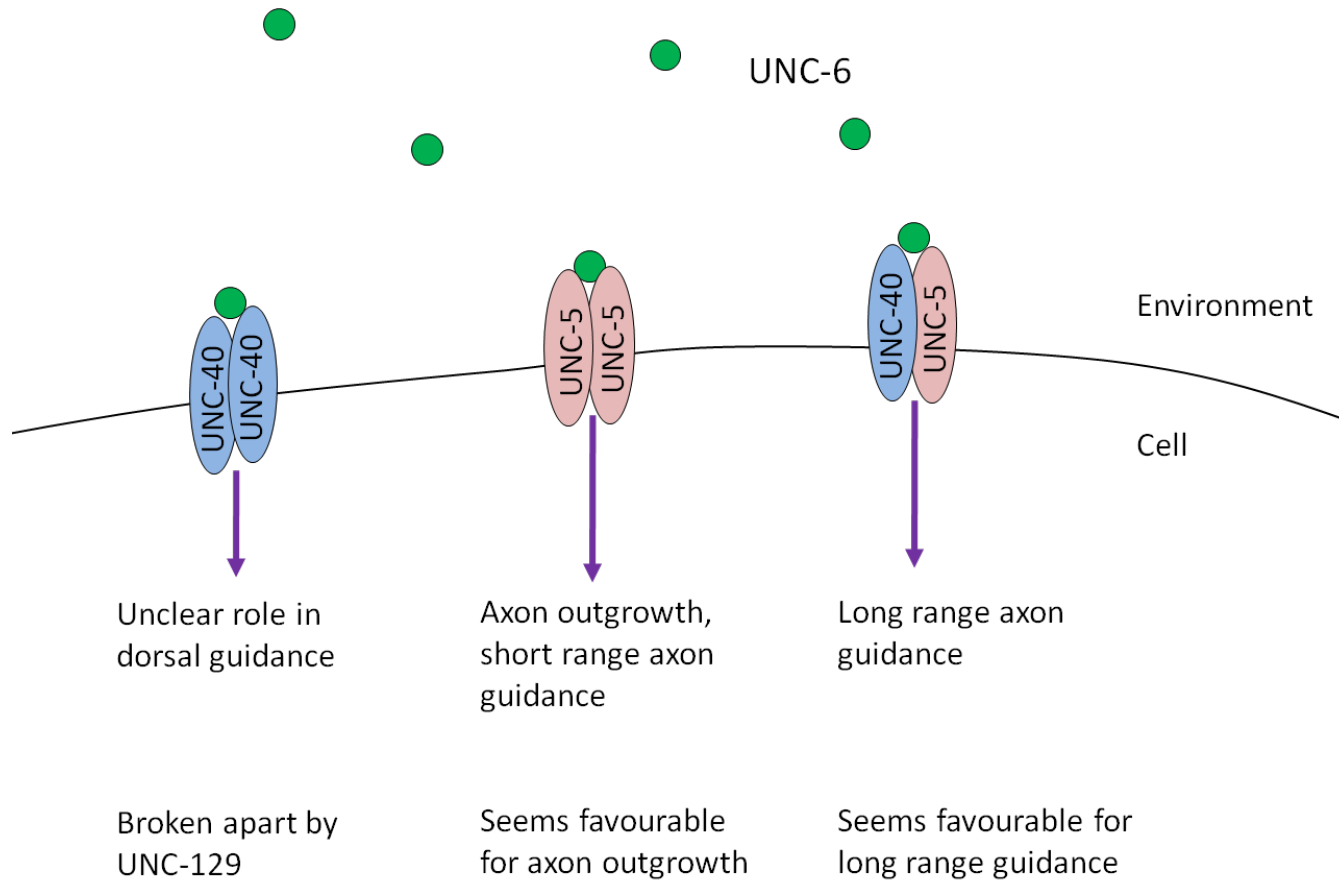
Figure 4.1: The current model for upstream signalling controlling axon outgrowth and guidance in the DA and DB motorneurons. UNC-5 and UNC-40 are the two known receptors in the UNC-6/Netrin signalling pathway. UNC-5 and UNC-40 can exist as homodimers with themselves or as heterodimers as an UNC-5/UNC-40 complex.

4.2   ENU-3, UNC-40 and SRC-1

To our surprise, *enu-3(tm4519)* was able to enhance the ventral guidance defects of the mechanosensory neurons that are observed in *unc-40(e1430)*. At the time, we did not expect ENU-3 to play a role in ventral guidance as the screen was conducted to discover enhancers of dorsal guidance. The enhancement of defects was quite significant and thus proves that ENU-3 is functioning in a pathway parallel to UNC-40. More importantly, the double mutant with *unc-6(ev400)* did not have enhanced ventral guidance defects, thus suggesting that ENU-3 functions downstream of UNC-6. UNC-40 appears to be the only receptor functioning directly downstream of UNC-6 for ventral guidance. However, in the absence of UNC-40, the number of defects is less than the number of defects in the absence of UNC-6, suggesting redundancy and an alternate pathway downstream of UNC-6. Since the defects in the *unc-40(e1430);enu-3(tm4519)* equal the defects observed in the double with *enu-3(tm4519);unc-6(ev400)*, it appears that we have disabled the alternative/redundant pathway downstream of UNC-6. This observation suggests that ENU-3 could be a co-receptor with UNC-40 for UNC-6.

UNC-40 has been known to play a role in directing the migration of many different cells and axons within the worm, including gonad migration, axon guidance and muscle arm development. Interestingly, *enu-3(tm4519)* or *enu-3(rq1)* did not have any gonad migration defects, but the *unc-40(e1430);enu-3(tm4519)* double mutant had gonad migration defects where a significant enhancement was observed in posterior gonads that failed to make the dorsal turn (Table 3.9). Studies have shown that UNC-5 expression is likely to be responsible for this turn (Su et al., 2000; Killeen et al., 2002). However, mutants in *unc-40* also have distal tip cell defects. Why is it that null *unc-40* mutants possess distal tip cell defects when making the turn? Why does the absence of ENU-3 enhance these defects? It can be postulated that something is

happening with respect to UNC-5. UNC-5 is expressed in the distal tip cell and is able to perform the dorsal migration based on its ability to respond to chemorepulsion by UNC-6 signalling. Over-expression of UNC-5 has been shown to cause the gonad to migrate dorsally before it has completed the intended longitudinal extension (Su et al., 2000). Mutations in *enu-3* failed to enhance the distal tip cell defects of *unc-5(e53)* and *unc-6(ev400)* but not *unc-40(e1430)* (Table 3.9). This is further support for the idea that ENU-3 could be an UNC-40 co-receptor.

Binding of UNC-6 to UNC-5 and UNC-40 receptors leads to phosphorylation of the receptors by tyrosine kinases (Tong et al., 2001; Killeen et al., 2002). Mutations to these phosphorylation sites have been shown to affect axon and distal tip cell guidance (Killeen et al., 2002). Previous work has shown that SRC-1, a receptor tyrosine kinase, plays a role immediately downstream of UNC-40 and is involved in axon guidance and distal tip cell migration (Li et al., 2004, Liu et al., 2004, Ren et al., 2004). Lee et al. (2005) showed that SRC-1 is able to control UNC-5 signalling by directly binding to the SH2 domain of UNC-5 and causing phosphorylation of UNC-5. In wild-type animals, UNC-5 is asymmetrically activated on cells along the presumptive UNC-6/Netrin gradient (Lee et al., 2005). This asymmetrical activation leads to polarization and ultimately repulsive guidance of the cells expressing UNC-5 (Lee et al., 2005). Interestingly, UNC-40 has been shown to interact with FAK and SRC (Li et al., 2004, Liu et al., 2004). This interaction with UNC-40 appears to be crucial in order to elicit UNC-6 attraction. This idea is quite confusing as UNC-40, which is normally involved in attraction to UNC-6, could thus be indirectly causing activation of UNC-5 to allow for repulsion of UNC-6.

The original idea that UNC-40 is only involved in UNC-6/Netrin mediated attraction is constantly evolving. UNC-40 now appears to play a role in both attraction and repulsion based on its properties to signal downstream to receptor tyrosine kinases such as SRC-1 and receptor

78

tyrosine phosphorylases such as CLR-1 (Chang et al., 2004, Lee et al., 2005). Depending on the other molecules that are recruited and if UNC-5 is activated, attraction or repulsion may or may not be an end result.

Based on our data, I have postulated a speculative mechanism of UNC-6 signalling with respect to CLR-1, SRC-1 and ENU-3 for both short range guidance/axon outgrowth and for long range guidance (Figure 4.2, 4.3, 4.4 and 4.5). UNC-5 could be inactive until activated by UNC-40 which has been activated by SRC-1. Once UNC-5 is phosphorylated and physically interacts with SRC-1, downstream signalling can be performed to elicit axon outgrowth and short range guidance (Figure 4.2). Once axon outgrowth and short range guidance have been performed, UNC-5/UNC-40 signalling probably takes over. I postulate that UNC-40 activated CLR-1 is dephosphorylating the UNC-5/SRC-1 complex and is either deactivating or hindering the ability of this complex to signal downstream (Figure 4.3). With respect to long range guidance, UNC-129 has been shown to disocciate the UNC-5 homodimers (Figure 4.4) (MacNeil et al., 2009). I believe that ENU-3 or some other molecule is breaking up the UNC-40 homodimers and allowing formation of the UNC-5/UNC-40 heterodimers (Figure 4.5). I postulate that CLR-1 is also playing some role in long range guidance by dephosphorylating the UNC-5 monomers and thus affecting the total amount of free activated UNC-5 that is available to bind to UNC-40. By controlling the amount of activated UNC-5, perhaps it may assist in the fine navigational decisions the growth cone needs to perform in order to reach its final target. Further biochemical analysis will need to be performed in order to compare and determine if there actually are two forms (phosphorylated and dephosphorylated) of the UNC-5/UNC-40 heterodimer complex and their respective activities.

It has been established that SRC-1 has the ability to activate UNC-5 through UNC-40 signalling, however there must be another mechanism controlling the localization and organization of UNC-5 and UNC-40 receptors on the surface of the cells. I postulate that ENU-3 is able to affect the localization of these axon guidance molecules. By controlling the positioning of the receptors on the cell surface, axon outgrowth, guidance and distal tip cell defects can be affected. Based on the idea that ENU-3 is somehow 'theoretically' acting upstream of UNC-40 by controlling localization of the UNC-5 and UNC-40 receptors, ENU-3 is perhaps partially responsible for positioning UNC-40 receptors correctly on the AVM and PVM cell bodies. It has been shown that UNC-40 is localized on the HSN cell body at the site of axon outgrowth (Addler et al., 2006., Chang et al., 2006, Quinn et al., 2008). In the absence of ENU-3, UNC-40 mutants more frequently projected axons which moved towards the head or moved dorsally. Perhaps UNC-40 receptors are mis-localized and are positioned at the sides of the cell which are dorsal or anterior with respect to the animal and thus cause the observed axon guidance defects. If this idea is true, this would account for all of the axon outgrowth and guidance defects observed in the DA and DB motorneurons, as well as the selective enhancement of the distal tip cells. This idea seems promising due to ENU-3's weak homology to cytoskeletal proteins (Section 3.9).

Although not included in this thesis, it was previously observed that *enu-3(rq1)* and *enu-3(tm4519)* mutants possess increased levels of physiological apoptosis in the germ line (Naqvi, 2010). In N2 animals, apoptosis of cells in the transition region of the gonad are uncommon (approximately 2 per gonad arm, n>200). In *enu-3* mutants the number of apoptotic corpses is doubled (approximately 4 per gonad arm). Recent research has shown that engulfment of apoptotic cells is mediated by integrin-α/SRC signalling (Hsu & Wu, 2010). SRC-1 provides a FAK-independent linkage between integrin-α and the CED-2/CED-5/CED-12 signalling module

to mediate engulfment of apoptotic corpses (Hsu & Wu, 2010). ENU-3 may be signalling

downstream to SRC-1 in addition to its proposed role, thus mutations to *enu-3* may affect

apoptotic cell engulfment. I have also shown that the level of apoptosis in *enu-3(rq1)* mutants is

not increased as a result of DNA damage. Therefore *enu-3* may be a pro-apoptotic factor and

thus a potential tumour suppressor which is an exciting prospect for future research.
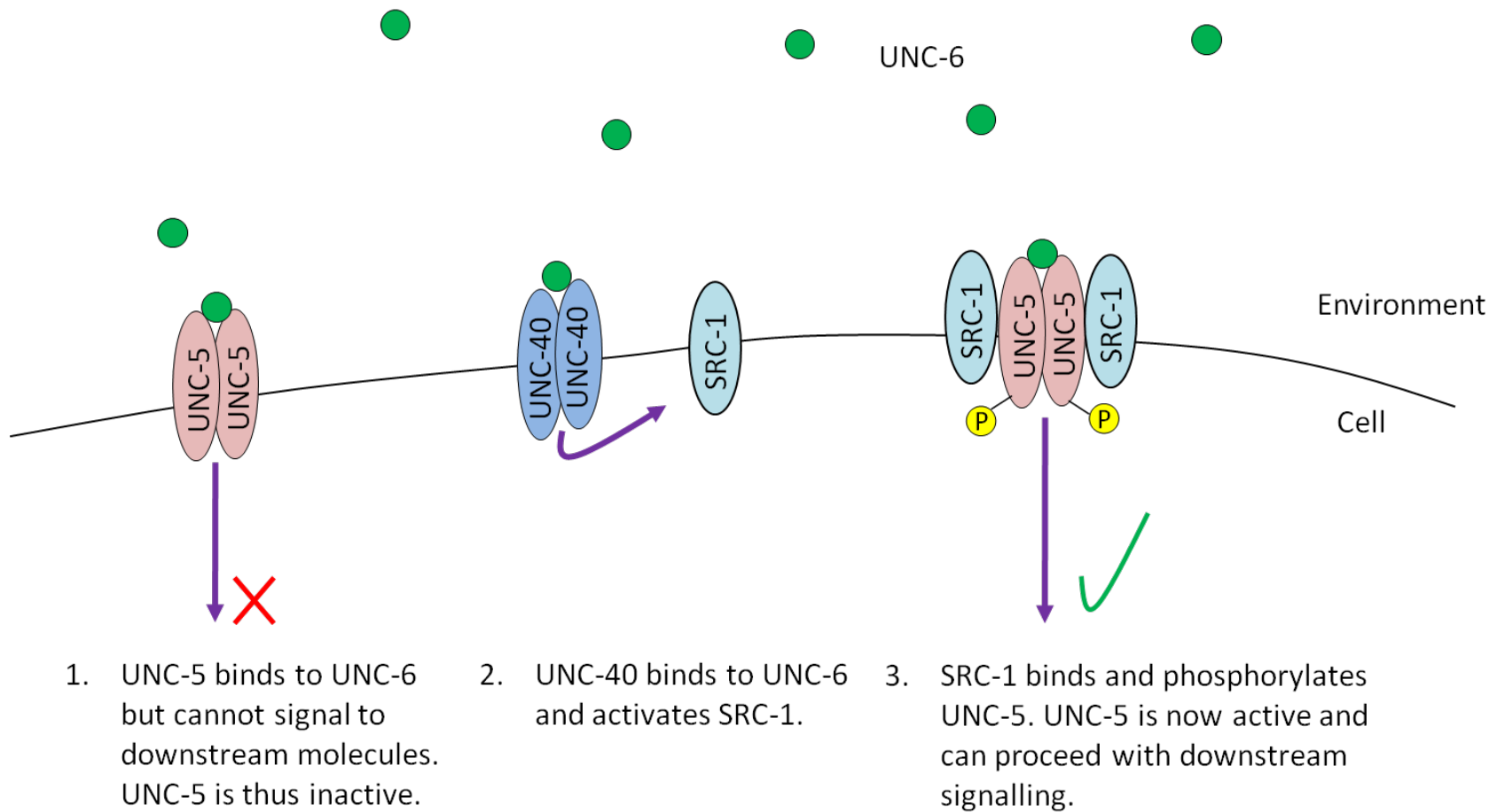
Figure 4.2: Positive regulation of UNC-5 signalling by UNC-40 activated SRC-1.

It can be hypothesized that UNC-5 is unable to signal downstream unless it is activated by a receptor tyrosine kinase such as SRC-1.

UNC-40 homodimers bind UNC-6 and subsequently activates SRC-1. SRC-1 is then able to bind and phosphorylate UNC-5.
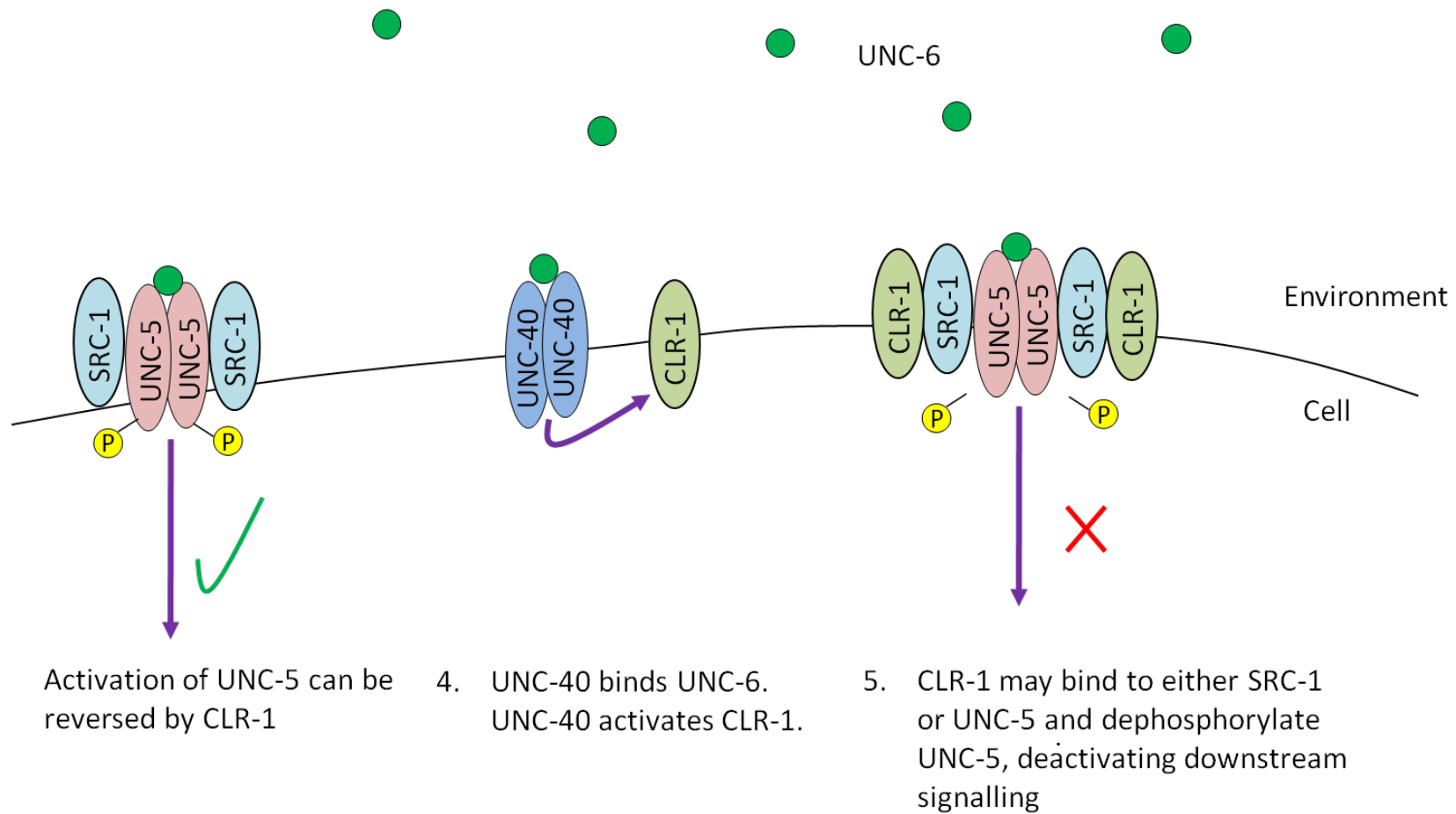
Figure 4.3: Negative regulation of UNC-5 signalling by UNC-40 activated CLR-1.

When axon outgrowth and short range guidance is complete, UNC-5 can possibly be deactivated by de-phosphorylation. UNC-40 homodimers bind UNC-6 and subsequently activates CLR-1. CLR-1 binds to the UNC-5 complex and de-phosphorylates UNC-5.
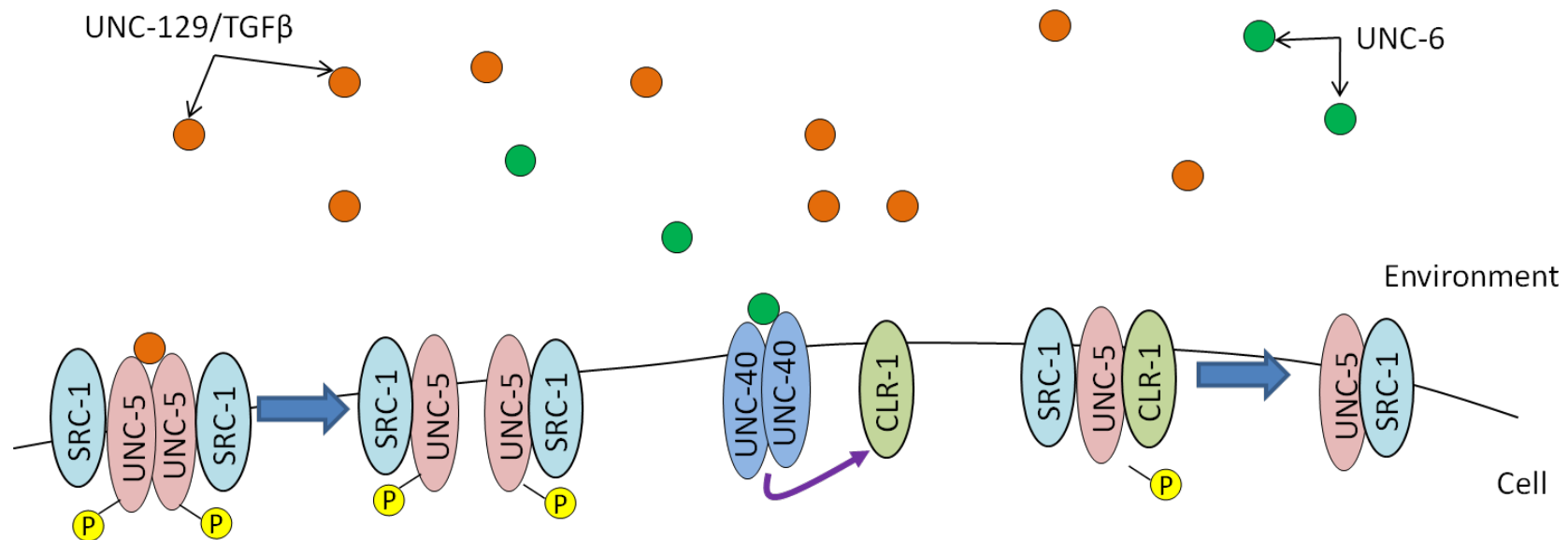
1. UNC-129 binds to the UNC-5 homodimers complex. UNC-129 breaks up the UNC-5 homodimers. It is unknown if SRC is still able to bind to UNC-5 after this breakage, but can be assumed.

2. UNC-40 homodimers bind UNC-6 and activate the receptor tyrosine phosphatase, CLR-1. CLR-1 dephosphorylates UNC-5 and can thus regulate the amount of activated UNC-5/SRC-1 present

Figure 4.4: UNC-129 breaks apart UNC-5 homodimers and CLR-1 controls the amount of activated UNC-5 present.

UNC-129 is expressed in a gradient opposite to UNC-6 and breaks apart UNC-5 homodimers. UNC-40 activated CLR-1 can then

dephosphorylate some of the UNC-5 units and switch them into an inactive or less active state.

3. ENU-3 binds to UNC-40 and can assist in breaking up or preventing the formation of UNC-40 homodimers

4. UNC-40 is now free to form heterodimers with both activated and unactivated UNC-5

5. The UNC-5/UNC-40 activated heterodimer can elicit long range guidance.
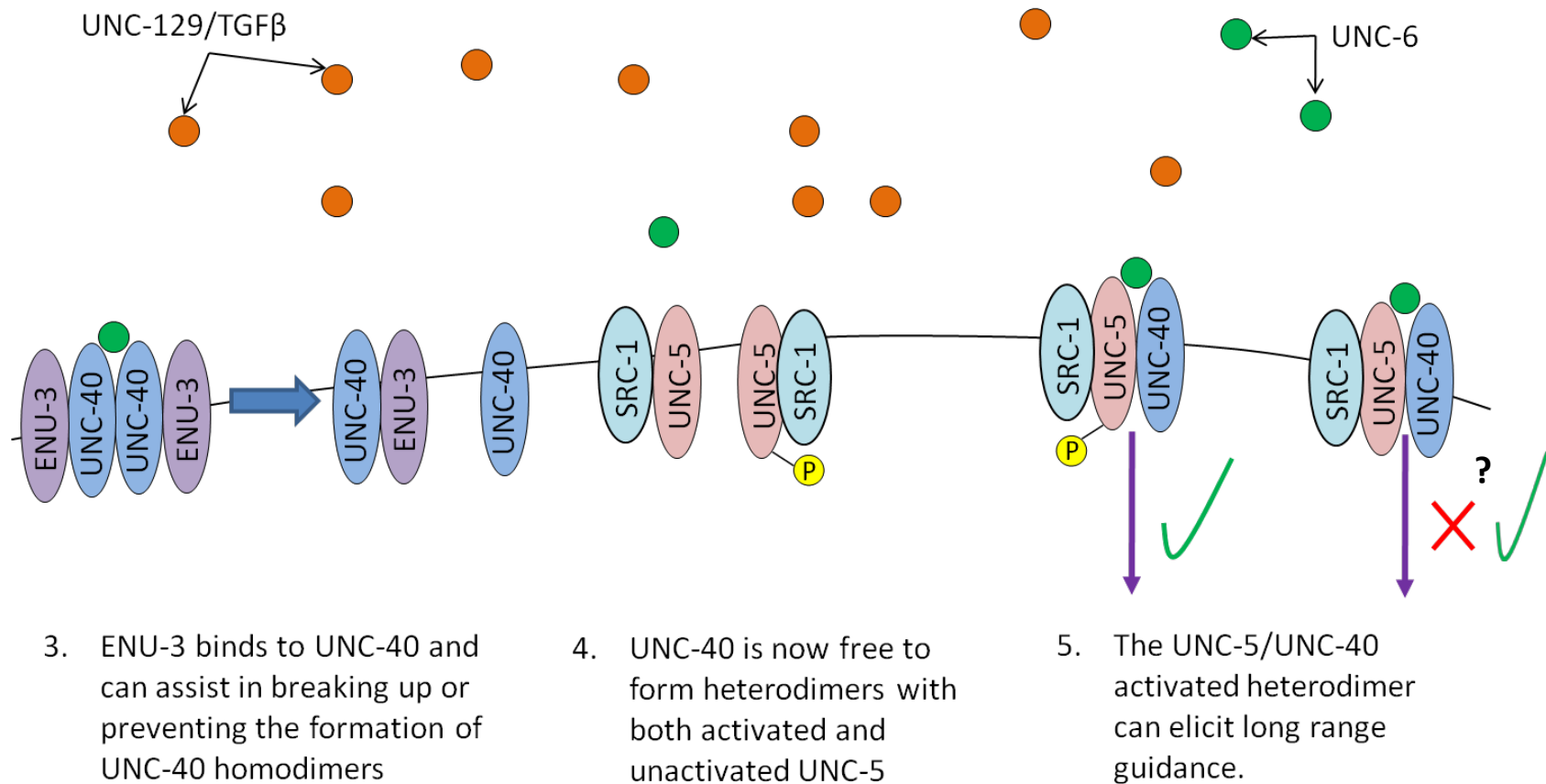
Figure 4.5: ENU-3 assists in preventing UNC-40 homodimer formation and encourages UNC-5/UNC-40 heterodimer formation

UNC-40 assists in either breaking up or preventing UNC-40 homodimer formation. UNC-40 is now free to bind to both inactive and active forms of UNC-5. Having both the fully active and the less active UNC-5 may be a key to controlling long range guidance mechanisms

4.3　　　ENU-3 interacts with GEI-4 and ZEN-4

GEI-4 and ZEN-4 are two well characterized proteins that play major roles in early development of the worm. Yeast-two-hybrid screens searching for interactors of these molecules were conducted and H04D03.1/ENU-3 was detected to have a physical interaction with both proteins (Li et al., 2004). Since ENU-3 interacts with GEI-4, a model can be generated involving ENU-3 in downstream signalling pathways (Figure 4.6).

4.3.1　　GEI-4

GEI-4 (GEX Interacting protein) is encoded by 9 different transcripts generating proteins that range from 174 to 564 amino acids. GEI-4 has been shown to physically interact with GEX-2 (Gut on Exterior) and appears to be responsible for embryonic viability, fertility and vulval morphogenesis (Tsuboi et al., 2002). GEX-2 is of interest as it was recently shown that GEX-2 functions downstream of the major axon guidance signalling pathways (Shakir et al., 2008). GEX-2 encodes a human homologue of Sra-1, which is a ligand for the small GTPase Rac1 in mammals (Soto et al., 2002). GEX-2 functions through the WAVE pathway, ultimately leading to filopodia extension of the growth cone (Shakir et al., 2008). Although this interaction may seem significant, it is unlikely that the interaction with ENU-3 fits in with our idea of what the protein is actually doing.

Based on our data, it is likely that ENU-3 is playing a role upstream of GEX-2 and that the interaction with GEI-4 may be contributing towards an unknown role of ENU-3. ENU-3 mutants did exhibit some signs of embryonic lethality and *enu-3(tm4519)* mutant males were generally infertile, supporting this idea of an alternative role. The GEX-2/GEX-3/GEI-4 protein

complex has further been shown to be crucial for proper regulation of intermediate filaments (IFs) during cytoskeletal rearrangement during embryogenesis (Tsuboi et al., 2002).

4.3.2   ZEN-4

ZEN-4 (Zygotic epidermal Enclosure defective) has 5 different transcripts generating proteins that range from 42 amino acids to 775 amino acids. ZEN-4 acts early on during development, appearing at the 2-cell stage and has been shown to be required for polar body extrusion after meiotic divisions, for completion of cytokinesis after mitosis, and for formation and maintenance of spindle midzone microtubules (Raich et al., 1998).

ZEN-4 appears to be a key molecule with respect to meiotic and mitotic divisions and also has been shown to resemble a kinesin-like protein (Raich et al., 1998). Kinesin has the ability to perform these tasks and is able to travel along microtubules in an ATP dependent process (Siddiqui et al., 2002). Besides kinesin's known roles in mitosis and meiosis, kinesins have also been shown to play a role in axonal transport (Etchberger et al., 2007). Kinesin is able to transport cellular molecules such as neurotransmitters and receptors from within the cell to the periphery (Etchberger et al., 2007). The relationship to ENU-3 and ZEN-4 remains unclear.
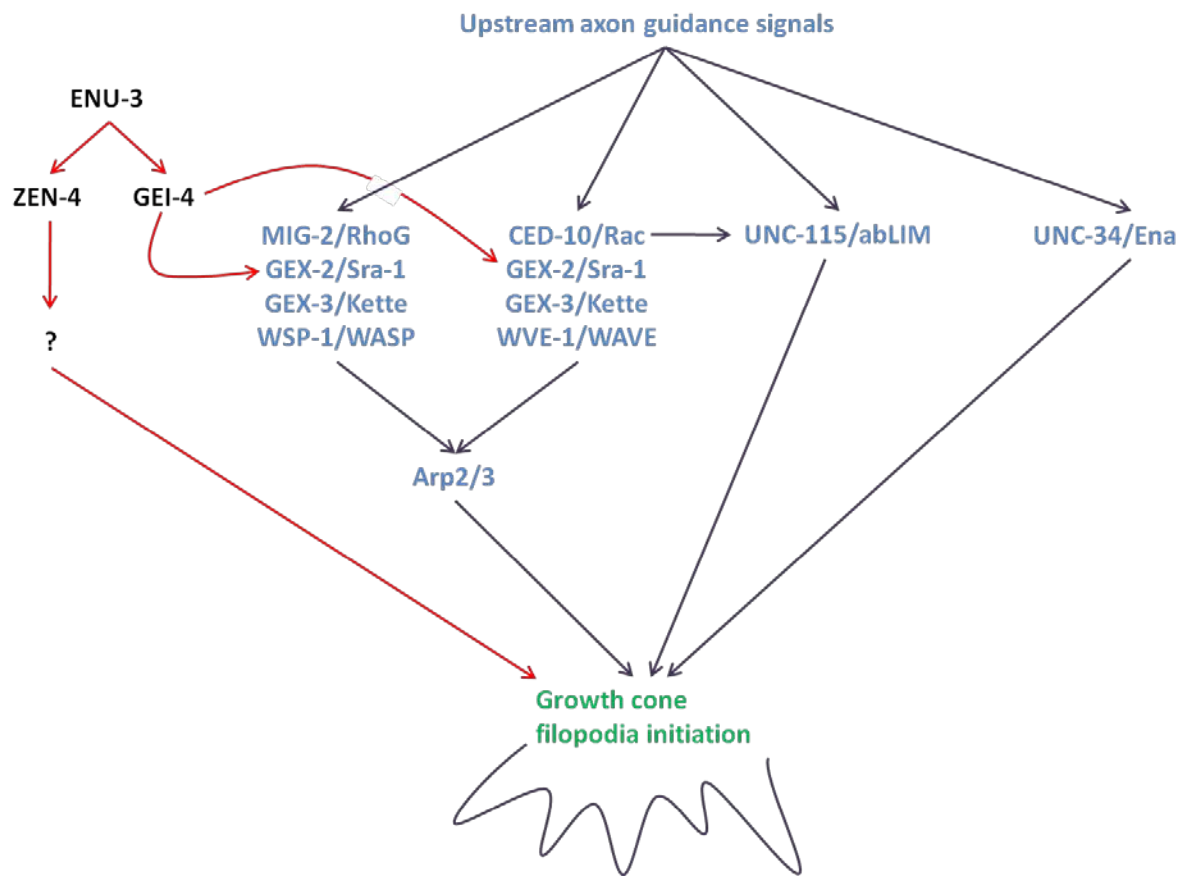
Figure 4.6: ENU-3 may play a role in downstream axon guidance signalling. There are currently four established pathways which can lead to growth cone filopodia initiation in *C. elegans*. ENU-3 has been shown to interact with two proteins, ZEN-4 and GEI-4. GEI-4 is known to interact with GEX-2 and thus ENU-3 may fit into the current model of downstream signalling (After Norris et al., 2009).

4.4   ENU-3 may play a role in cytoskeletal rearrangement

In rare cases it was observed that L4 and older animals of the *enu-3(tm4519);unc-40(e1430)* strain had broken or snapped axons that have undergone remodelling and repair. In some cases, the neurons appeared to be quite messy, tangled, or failed to reconnect at the point where the axons had snapped. This result suggests that ENU-3 may play a role in axon structural stability or integrity of the cytoskeleton. The axon breaking phenotype resembled the phenotype of the Spectrin mutants. In *C. elegans*, *unc-70* encodes β-Spectrin. Mutations in *unc-70* result in increased axon outgrowth defects and snapped axons of the VD and DD motorneurons (Hammarlund et al., 2000; Hammarlund et al., 2007). As a result, the animals are extremely uncoordinated and have shortened body length (Hammarlund et al., 2007). However, due to the structural predictions, it is highly unlikely that ENU-3 plays a role in direct downstream signalling of the conserved pathways of axon guidance. However, the authors of the original *unc-70* papers did not examine the DA and DB motorneurons. It would be interesting to place a marker for these neurons in the *unc-70* mutants to study axon outgrowth defects. It seems unlikely that a double mutant between *enu-3* and *unc-70* would cause increased axon outgrowth defects in *unc-5(e53)* as UNC-70 is most likely extremely far downstream of UNC-5 but the idea can now be tested.

Although the *enu-3* mutants possess some similarity with respect to defects observed in these Spectrin mutants, the more interesting story with respect to cytoskeletal rearrangement lies with GEI-4. GEI-4 mutants have not been shown to possess axon guidance defects, tempting us to speculate if ENU-3 may be acting both upstream and downstream of the known axon guidance pathways.

89

4.5   Future Experiments

Despite the progress that has been made with respect to understanding ENU-3, there is

still a cloud of uncertainty with respect to its molecular function and the role it plays in

development of the worm. I present in this section various genetic and biochemical analyses that

will hopefully be performed by future researchers in the years to come.

4.5.1   Another Genetic Enhancer Screen

It is likely that most of the major axon guidance molecules have already been identified

and that the proteins that researchers are identifying today are the 'second tier' proteins

functioning downstream of the larger, more important known molecules. The original screen to

identify ENU-3 was performed by EMS mutagenesis in an *unc-5(e53)* background. The goal of

the screen was to obtain mutants that had a 100% of axon outgrowth defects in the DA and DBs.

Unfortunately these animals were extremely sick and were not considered practical candidates to

continue further analysis. Instead, a mutant named *rq1* which had slightly enhanced axon

outgrowth defects, was selected.

Although *rq1* did prove to be a true enhancer of *unc-5(e53)* and is the key discovery

regarding my research in my thesis, it was not an ideal allele to be pulled from the screen as

penetrance of the defects was not 100%. Instead, I propose that the screen should be repeated.

Instead of picking semi-viable mutants, the extremely sick mutants should be picked and

maintained as heterozygotes. Although not simple, this would increase the chances of

discovering a more significant, upstream gene involved in axon outgrowth. Once the mutation is

roughly mapped, the mutation can be carried by a balancer and maintained efficiently (Riddle et

al., 1997).

90

4.5.2 Localization Experiments

If the hypothesis regarding ENU-3 being able to orient axon guidance receptors to certain parts of the cell holds true, localization experiments will provide conclusive evidence. These experiments are relatively simple since many integrated lines of translational fusions of various axon guidance molecules are readily available to the worm community. These experiments simply entail crossing these reporter fusion constructs into the *enu-3(tm4519)* mutant and observing the expression pattern using epifluorescence. To allow for scoring these lines should also possess a marker for a pan-neuronal and or a distal tip cell marker depending on the phenotype being examined. It would be interesting to see if there is mislocalization of UNC-5::GFP and or UNC-40::GFP in the mutant, as well as whether the cells that possess these mislocalization flaws also have axon migration defects. If so, it is almost certain that the observed axon migration defects can be attributed to mislocalization of the protein under scrutiny.

4.5.3 Yeast-Two-Hybrid Screen

As *enu-3* has already been positionally cloned, it would be interesting to see and validate that the two interactors, GEI-4 and ZEN-4, actually interact with ENU-3. In addition to these proteins, I expect a variety of cytoskeletal proteins and possibly UNC-40 and UNC-5 to be revealed as hits. Performing two-hybrid screens on transmembrane proteins can be quite tricky, but recent methods performed and optimized by Stagljar's group at the University of Toronto have shown to be successful.

4.5.4 ENU-3 and the paralogs of ENU-3

Other experiments that need to be performed are centered upon the paralogs of ENU-3. In *C. elegans*, there are four close protein paralogs that strikingly resemble ENU-3 at the amino acid level (Figure 4.1). *enu-3* is most likely to be the result of an ancestral deletion and translocation and these other larger paralogs could play a much larger role in development than ENU-3. Mutant alleles, preferably null, need to be generated for these genes and have been requested from the knock-out facility of the Mitani group. The mutants should then be crossed with null alleles of *unc-5, unc-6* and *unc-40* and assessed for their ability to enhance axon outgrowth and guidance defects. As I mentioned earlier, preliminary RNAi data suggest that the knockdown of these paralogs generate enhanced axon outgrowth defects in the background of *unc-5(e53)*. Thus, the likelihood of these genes behaving in the same fashion as *enu-3* is highly likely.

It would be interesting to investigate the expression pattern of the paralogs through the use of transcriptional and translational reporters. ENU-3 was found to be expressed in a wide variety of tissues, primarily neuronal and muscular. If the paralogs have similar expression patterns, this would further support the idea that they are behaving like ENU-3 and that they are playing some sort of redundant role/function. Despite expression in both the DA and DB sets of motor neurons, ENU-3 was found to only play a major role in DB motorneurons with respect to axon outgrowth. Knockdown of one of the paralogs, W0F52.2, was recently shown to affect motor axon outgrowth of the DA motorneurons. It could be possible that ENU-3 is only playing a minor guidance role in the DA motorneurons, while playing a major role during axon outgrowth of the DB motorneurons. Perhaps performing RNAi experiments in the double mutant background, *enu-3(tm4519);unc-5(e53),* will generate enhanced axon outgrowth defects of the

DA motorneurons. However, if there is no enhancement of the motor axon outgrowth defects, it could suggest that the paralog being tested is functioning downstream of the UNC-6/Netrin pathway or downstream of an unknown ENU-3 pathway. Indeed, much more work needs to be conducted with respect to understanding the function of the paralogs by performing various expression and RNAi experiments. It would be interesting to see if simultaneous knockdown of all of the paralogs would result in no axon outgrowth of the DA and DBs.

Microinjection experiments should be performed by injecting wild-type genomic copies of the paralogs into *enu-3* mutants and scoring for rescue. I postulate that a dosage effect may occur and that the paralogs may be able to rescue the defects of these mutants. If so, dosage experiments could be conducted. Constructs could be constructed where promoters of different expression levels could be used to drive expression of ENU-3 and its paralogs and scored for rescue in the DA and DB motorneurons. Although the screen was conducted screening for genetic enhancers in these two sets of cells, pan-neuronal promoters should also be used in order to observe the effect of ENU-3 and these other proteins elsewhere. I believe that the new family of proteins that we have discovered will play a major role in guidance of many tissues and neurons in the worm. The role of these proteins (if any) in higher organisms is more difficult to speculate as the true homologies are not clear. ENU-3 has weak homology with human hydin, a protein implicated in hydrocephaly but the significance is not clear.

4.5.5   Biochemistry

Although a great tool, biochemical experiments in *C. elegans* are difficult as extraction poses a challenge and the sizes of the neuronal cells are quite small. Nonetheless, I will discuss future biochemical experiments that should be conducted on ENU-3 in the future.

Firstly, integrated lines with varying expression of ENU-3 fused to an epitope tag must be constructed. The original expression lines were conducted as ENU-3::GFP but should be constructed with a more robust tag as many other worm reagents use GFP as a marker. Using an alternative such as Kaede or dsRed2 would allow for easy visualization using epifluorescence. As I mentioned in the previous paragraph, motor neuron cell bodies are quite small and to observe sub-cellular localization is very difficult. To circumvent this issue, a larger cell model should be used such as a cell culture system. Mammalian cell lines expressing ENU-3::GFP would provide clear resolution and give an idea as to where ENU-3 is localized within the cell.

Once the mammalian lines expressing ENU-3 fusion proteins are made, a variety of experiments could be performed. A key experiment that I would like to see performed would be an attempt at the co-immunoprecipitation of ENU-3 with UNC-40. I doubt if ENU-3 binds directly to UNC-6 and more likely works together with UNC-40. If UNC-40 does co-precipitate with the ENU-3, further investigation should be performed regarding the interaction between the two proteins. Are they interacting directly or indirectly? In any case, mass spectroscopy should be performed by performing an ENU-3 "pull-down". ENU-3 could be tagged with a TAP tag, as TAP tags can be cleaved off after purification in order to preserve protein integrity. The resulting protein complex could be thus analyzed and hopefully reveal interactors of known composition, and thus known identity.

Chapter 5.   Conclusions

The development of the nervous system is a delicate, intricate and fascinating process where neuronal molecules are able to communicate and cross-talk with one another in order to generate the identical structures in almost every single multicellular organism. The power of genetics is fascinating and the programmed development of the nervous system even more. Understanding the UNC-6/Netrin pathway and searching for genes that function parallel to known signalling pathways is an exciting field and the discovery of ENU-3, a novel protein, will hopefully further contribute to our understanding of neuronal development. The work in this study has identified and characterized *enu-3* using a genetic approach and has shown that *enu-3* appears to be involved in both axon outgrowth and guidance of the DA and DB motorneurons, as well as have some general axon guidance abilities in other neurons such as the AVM and PVM. ENU-3 appears to have two known interactors, ZEN-4 and GEI-4, which appear to be involved in cytoskeletal rearrangement. ENU-3 also possesses 4 closely related paralogs which appear to resemble ENU-3 with respect to function. Future work should be conducted in order to determine the exact biochemical function and role of ENU-3 not only in the nervous system, but also in development of the animal as a whole.

Chapter 6.   Supplementary Information

In this section I describe in detail the conditions used to generate the PCR products that were used for the microinjection rescue and expression pattern experiments. The construction of the transcriptional fusion, the translational fusion and the cell autonomy/unc-129 rescue construct are described below.

6.1   Transcriptional Fusion

Approximately 3kb of the promoter of *enu-3* was used to drive the transcriptional fusion. Using Roche Long Template Expand System 2, 3kb was amplified. 80 ng of the H04D03 fosmid was obtained and used as template to amplify the promoter of H04D03.1. Two primers were used for the first amplication; "Outside H04D03.1" was used as the upstream primer and "Transcriptional Fusion" was used as the downstream primer. For the fusion reaction two different primers were used; "Nested H04D03.1" was used as the upstream primer and "GFP Nested" was used as the downstream primer. The primers and PCR conditions are listed below (Table 6.1, Table 6.2, Table 6.3, Table 6.4 and Table 6.5).

Primer Name	Sequence
Outside H04D03.1	CGT-GTA-ACT-CCT-TTC-ATC-TTG-GCA-ACC-ATA-GCT-CCG
Nested H04D03.1	CTG-TTG-AAG-GAG-ATC-CTC-TTT
Transcriptional Fusion	AGT CGA-CCT-GCA-GGC-ATG-CAA-GCT-GAG-TAG-GGG CAG-GGA-CTA-T
GFP Nested	GGA-AAC-AGT-TAT-GTT-TGG-TAT-A

Table 6.1: List of primers used to generate the *enu-3* transcriptional fusion

Component	Volume
dNTP (500 uM each, mixed)	2.5 uL
Upstream Primer (300 nM)	1 uL
Downstream Primer (300 nM)	1 uL
10x PCR buffer (System 2)	5 uL
Template DNA (fosmid DNA)	1 uL (80 ng)
Expand Long Template Enzyme Mix	0.75 uL
ddH$_2$O	38.75 uL

Table 6.2: Components of PCR mixture to amplify the promoter of *enu-3*.

Step	Temperature	Time	Cycles
Initial Denaturation	94°C	2 min	1
Denaturation	94°C	10 s	10
Annealing	55°C	30 s	
Elongation	68°C	2 min	
Denaturation	94°C	15 s	25
Annealing	55°C	30 s	
Elongation	68°C	2 min + 20 s cycle elongation for each successive cycle	
Final Elongation	68°C	7 min	1
Cooling	4°C	Unlimited Time	-

Table 6.3: PCR Conditions that were used to amplify the promoter of *enu-3*.

The resulting PCR product was run on a 0.7% agarose gel and a product of 3kb was obtained. The GFP product that was described earlier on was estimated on the same gel and approximately equal quantities of the GFP product and the promoter product were used for the fusion reaction (80ng each) with TaKaRa Ex Taq.

Component	Volume
dNTP TaKaRa Mixture (2.5 mM each)	4 uL
Upstream Primer (300 nM)	1 uL
Downstream Primer (300 nM)	1 uL
10x Ex Taq Buffer	5 uL
Promoter PCR Product	1 uL (80 ng)
GFP PCR Product	1 uL (80 ng)
TaKaRa Ex Taq (5 units/uL)	0.25 uL
ddH$_2$O	36.75 uL

Table 6.4: Components of the PCR fusion mixture to generate *enu-3p::gfp*.

Step	Temperature	Time	Cycles
Initial Denaturation	98°C	2 min	1
Denaturation	94°C	10 s	30
Annealing	55°C	30 s	
Elongation	72°C	5 min	
Final Elongation	72°C	10 min	1
Cooling	4°C	Unlimited Time	-

Table 6.5: PCR Conditions that were used to generate the *enu-3p::gfp* fusion construct

6.2   Translational Fusion

Approximately 3kb of the promoter of *enu-3* was used to drive the translational fusion. The H04D03.1 gene is approximately 1kb. Using Roche Long Template Expand System 2, 4kb was amplified. 80 ng of the H04D03 fosmid was obtained and used as template to amplify the promoter and gene of H04D03.1. Two primers were used for the first amplication: "Outside H04D03.1" was used as the upstream primer and "Translational Fusion" was used as the downstream primer. For the fusion reaction two different primers were used; "Nested H04D03.1" was used as the upstream primer and "GFP Nested" was used as the downstream primer. The primers and PCR conditions are listed below (Table 6.6, Table 6.7, Table 6.8, Table 6.9 and Table 6.10).

Primer Name	Sequence
Outside H04D03.1	CGT-GTA-ACT-CCT-TTC-ATC-TTG-GCA-ACC-ATA-GCT-CCG
Nested H04D03.1	CTG-TTG-AAG-GAG-ATC-CTC-TTT
Translational Fusion	AGT-CGA-CCT-GCA-GGC-ATG-CAA-GCT-ATC-GCG-TGG-CTT-GTC-CAC-AGT
GFP Nested	GGA-AAC-AGT-TAT-GTT-TGG-TAT-A

Table 6.6: List of primers used to generate the *enu-3* translational fusion

Component	Volume
dNTP (500 uM each, mixed)	2.5 uL
Upstream Primer (300 nM)	1 uL
Downstream Primer (300 nM)	1 uL
10x PCR buffer (System 2)	5 uL
Template DNA (fosmid DNA)	1 uL (80 ng)
Expand Long Template Enzyme Mix	0.75 uL
ddH$_2$O	38.75 uL

Table 6.7: Components of PCR mixture to amplify the promoter and gene of *enu-3*.

Step	Temperature	Time	Cycles
Initial Denaturation	94°C	2 min	1
Denaturation	94°C	10 s	10
Annealing	55°C	30 s	
Elongation	68°C	4 min	
Denaturation	94°C	15 s	25
Annealing	55°C	30 s	
Elongation	68°C	4 min + 20 s cycle elongation for each successive cycle	
Final Elongation	68°C	7 min	1
Cooling	4°C	Unlimited Time	-

Table 6.8: PCR Conditions that were used to amplify the promoter and gene of *enu-3*.

The resulting PCR product was run on a 0.7% agarose gel and a product of 4kb was obtained. The GFP product that was described earlier on was estimated on the same gel and approximately equal quantities of the GFP product and the promoter product were used for the fusion reaction (80ng each) with TaKaRa Ex Taq.

Component	Volume
dNTP TaKaRa Mixture (2.5 mM each)	4 uL
Upstream Primer (300 nM)	1 uL
Downstream Primer (300 nM)	1 uL
10x Ex Taq Buffer	5 uL
Promoter PCR Product	1 uL (80 ng)
GFP PCR Product	1 uL (80 ng)
TaKaRa Ex Taq (5 units/uL)	0.25 uL
ddH$_2$O	36.75 uL

Table 6.9: Components of the PCR fusion mixture to generate *enu-3::gfp*.

Step	Temperature	Time	Cycles
Initial Denaturation	98°C	2 min	1
Denaturation	94°C	10 s	30
Annealing	55°C	30 s	
Elongation	72°C	6 min	
Final Elongation	72°C	10 min	1
Cooling	4°C	Unlimited Time	-

Table 6.10: PCR Conditions that were used to generate the *enu-3::gfp* construct.

6.3   *unc-129p::enu-3::gfp*

In order to test cell autonomy, a promoter known to express selectively in the DA and DB motorneurons was selected to drive expression of the *enu-3* gene fused to GFP. The Long Template Expand System 2 (Roche) was used to amplify both the promoter of *unc-129* (2.5 kb) and *enu-3::gfp* (3 kb). 30 ng of the pAC12 plasmid was obtained and used as template to amplify the promoter of *unc-129*. The pre-existing translational fusion was used as a template to amplify *enu-3::gfp* (20 ng).

Two primers were used to amplify the promoter of *unc-129*: "Outside *unc-129*" was used as the upstream primer and "*unc-129* Fusion" was used as the downstream primer. For the fusion reaction to fuse the two amplicons together, "Nested *unc-129*" was used as the upstream primer and "GFP Nested" was used as the downstream primer. The primers and PCR conditions are listed below (Table 6.11, Table 6.12, Table 6.13, Table 6.14, Table 6.15, Table 6.16 and Table 6.17).

Primer Name	Sequence
Outside *unc-129*	CAT-AAT-TTT-CGT-GGG-AAT-CTT-CGG
Nested *unc-129*	TGC-TCT-TTG-CGG-TTT-ATA-AGT-GGA
unc-129 Fusion	GAA-AAC-AAA-ATA-CGC-AAA-ATA-CGC-ATT-TTC-TTG-CTT-GCT-CTT-CCA-ATT-TTC-CT
enu-3::gfp Forward	ATG-CGT-ATT-TTG-CGT-ATT-TTG-TTT-TCA-TTG
GFP Nested	GGA-AAC-AGT-TAT-GTT-TGG-TAT-A

Table 6.11: List of primers used to generate the *unc-129p::enu-3::gfp* construct

Component	Volume
dNTP (500 uM each, mixed)	2.5 uL
Upstream Primer (300 nM)	1 uL
Downstream Primer (300 nM)	1 uL
10x PCR buffer (System 2)	5 uL
Template DNA (plasmid DNA)	1 uL (30 ng)
Expand Long Template Enzyme Mix	0.75 uL
ddH$_2$O	38.75 uL

Table 6.12: Components of PCR mixture to amplify the promoter of *unc-129*.

Step	Temperature	Time	Cycles
Initial Denaturation	94°C	2 min	1
Denaturation	94°C	10 s	10
Annealing	55°C	30 s	
Elongation	68°C	2 min	
Denaturation	94°C	15 s	25
Annealing	55°C	30 s	
Elongation	68°C	2 min + 20 s cycle elongation for each successive cycle	
Final Elongation	68°C	7 min	1
Cooling	4°C	Unlimited Time	-

Table 6.13: PCR Conditions that were used to amplify the promoter of *unc-129*.

The resulting PCR product was run on a 0.7% agarose gel and a product of 2.5 kb was obtained. To amplify the amplicon containing *enu-3::gfp* from the translational fusion, two primers were used: "*enu-3::gfp* Forward" was used as the upstream primer and "GFP Nested" was used as the downstream primer.

Component	Volume
dNTP (500 uM each, mixed)	2.5 uL
Upstream Primer (300 nM)	1 uL
Downstream Primer (300 nM)	1 uL
10x PCR buffer (System 2)	5 uL
Template DNA (PCR product)	1 uL (20 ng)
Expand Long Template Enzyme Mix	0.75 uL
ddH$_2$O	38.75 uL

Table 6.14: Components of PCR mixture to amplify *enu-3::gfp*.

Step	Temperature	Time	Cycles
Initial Denaturation	94°C	2 min	1
Denaturation	94°C	10 s	10
Annealing	55°C	30 s	
Elongation	68°C	2 min	
Denaturation	94°C	15 s	25
Annealing	55°C	30 s	
Elongation	68°C	2 min + 20 s cycle elongation for each successive cycle	
Final Elongation	68°C	7 min	1
Cooling	4°C	Unlimited Time	-

Table 6.15: PCR Conditions that were used to amplify *enu-3::gfp*.

The resulting PCR product was run on a 0.7% agarose gel and a product of 3 kb was obtained. To fuse the two amplicons, the *unc-129* promoter and the *enu-3::gfp* products, two primers were used; "Nested *unc-129*" was used as the upstream primer and "GFP Nested" was used as the downstream primer.

Component	Volume
dNTP TaKaRa Mixture (2.5 mM each)	4 uL
Upstream Primer (300 nM)	1 uL
Downstream Primer (300 nM)	1 uL
10x Ex Taq Buffer	5 uL
Promoter PCR Product	1 uL (80 ng)
enu-3::gfp PCR Product	1 uL (80 ng)
TaKaRa Ex Taq (5 units/uL)	0.25 uL
ddH$_2$O	36.75 uL

Table 6.16: Components of the PCR fusion mixture to generate *unc-129p::enu-3::gfp.*

Step	Temperature	Time	Cycles
Initial Denaturation	98°C	2 min	1
Denaturation	94°C	10 s	30
Annealing	55°C	30 s	
Elongation	72°C	6 min	
Final Elongation	72°C	10 min	1
Cooling	4°C	Unlimited Time	-

Table 6.17: PCR Conditions that were used to generate the *enu-3::gfp* fusion construct

Chapter 7. References

Adler, C. E., Fetter, R. D., & Bargmann, C. I. (2006). UNC-6/Netrin induces neuronal asymmetry and defines the site of axon formation. *Nature Neuroscience*, 9(4), 511-518.

Bagnard, D., Lohrum, M., Uziel, D., Puschel, A. W., & Bolz, J. (1998). Semaphorins act as attractive and repulsive guidance signals during the development of cortical projections. *Development (Cambridge, England), 125*(24), 5043-5053.

Brenner, S. (1974). The genetics of caenorhabditis elegans. *Genetics, 77*(1), 71-94.

Bueno de Mesquita M (2009). Characterization of *rq1*, a mutant involved in nervous system development in *C. elegans*. Masters thesis, Ryerson University library, Toronto.

Campbell, D. S., & Holt, C. E. (2001). Chemotropic responses of retinal growth cones mediated by rapid local protein synthesis and degradation. *Neuron, 32*(6), 1013-1026.

Chalfie, M., Sulston, J. E., White, J. G., Southgate, E., Thomson, J. N., & Brenner, S. (1985). The neural circuit for touch sensitivity in caenorhabditis elegans. *The Journal of Neuroscience : The Official Journal of the Society for Neuroscience, 5*(4), 956-964.

Chan, S. S., Zheng, H., Su, M. W., Wilk, R., Killeen, M. T., Hedgecock, E. M., et al. (1996). UNC-40, a C. elegans homolog of DCC (deleted in colorectal cancer), is required in motile cells responding to UNC-6 netrin cues. *Cell, 87*(2), 187-195.

Chang, C., Yu, T. W., Bargmann, C. I., & Tessier-Lavigne, M. (2004). Inhibition of netrin-mediated axon attraction by a receptor protein tyrosine phosphatase. *Science (New York, N.Y.), 305*(5680), 103-106.

Chang, C., Adler, C. E., Krause, M., Clark, S. G., Gertler, F. B., Tessier-Lavigne, M., et al. (2006). MIG-10/lamellipodin and AGE-1/PI3K promote axon guidance and outgrowth in response to slit and netrin. *Current Biology* : CB, 16(9), 854-862.

Chin-Sang, I. D., Moseley, S. L., Ding, M., Harrington, R. J., George, S. E., & Chisholm, A. D. (2002). The divergent *C. elegans* ephrin EFN-4 functions inembryonic morphogenesis in a pathway independent of the VAB-1 eph receptor. *Development (Cambridge, England), 129*(23), 5499-5510.

Colamarino, S. A., & Tessier-Lavigne, M. (1995). The axonal chemoattractant netrin-1 is also a chemorepellent for trochlear motor axons. *Cell*, 81(4), 621-629.

Colavita, A., & Culotti, J. G. (1998). Suppressors of ectopic UNC-5 growth cone steering identify eight genes involved in axon guidance in caenorhabditis elegans. *Developmental Biology, 194*(1), 72-85.

Colavita, A., Krishna, S., Zheng, H., Padgett, R. W., & Culotti, J. G. (1998). Pioneer axon guidance by UNC-129, a C. elegans TGF-beta. *Science (New York, N.Y.), 281*(5377), 706-709.

Dalpe, G., Zhang, L. W., Zheng, H., & Culotti, J. G. (2004). Conversion of cell movement responses to semaphorin-1 and plexin-1 from attraction to repulsion by lowered levels of

specific RAC GTPases in *C. elegans*. *Development (Cambridge, England), 131*(9), 2073-2088.

Desai, C., Garriga, G., McIntire, S. L., & Horvitz, H. R. (1988). A genetic pathway for the development of the caenorhabditis elegans HSN motor neurons. *Nature, 336*(6200), 638-646.

Etchberger, J. F., Lorch, A., Sleumer, M. C., Zapf, R., Jones, S. J., Marra, M. A., et al. (2007). The molecular signature and cis-regulatory architecture of a *C. elegans* gustatory neuron. *Genes & Development, 21*(13), 1653-1674.

Fraser, A. G., Kamath, R. S., Zipperlen, P., Martinez-Campos, M., Sohrmann, M., & Ahringer, J. (2000). Functional genomic analysis of *C. elegans* chromosome I by systematic RNA interference. *Nature, 408*(6810), 325-330.

Fujii, T., Nakao, F., Shibata, Y., Shioi, G., Kodama, E., Fujisawa, H., et al. (2002). Caenorhabditis elegans PlexinA, PLX-1, interacts with transmembrane semaphorins and regulates epidermal morphogenesis. *Development (Cambridge, England), 129*(9), 2053-2063.

Fujisawa, K., Wrana, J. L., & Culotti, J. G. (2007). The slit receptor EVA-1 coactivates a SAX-3/Robo mediated guidance signal in *C. elegans*. *Science (New York, N.Y.),317*(5846), 1934-1938.

Hammarlund, M., Davis, W. S., & Jorgensen, E. M. (2000). Mutations in beta-spectrin disrupt axon outgrowth and sarcomere structure. *The Journal of Cell Biology, 149*(4), 931-942.

Hammarlund, M., Jorgensen, E. M., & Bastiani, M. J. (2007). Axons break in animals lacking beta-spectrin. *The Journal of Cell Biology, 176*(3), 269-275.

Hao, J. C., Yu, T. W., Fujisawa, K., Culotti, J. G., Gengyo-Ando, K., Mitani, S., et al. (2001). *C. elegans* slit acts in midline, dorsal-ventral, and anterior-posterior guidance via the SAX-3/Robo receptor. *Neuron, 32*(1), 25-38.

Hall, D. H. & Altun, Z.F. (2008). *C. elegans* Atlas. Cold Spring harbor laboratory press (Cold Spring Harbour, New York), 62-70

Harris, R., Sabatelli, L. M., & Seeger, M. A. (1996). Guidance cues at the drosophila CNS midline: Identification and characterization of two drosophila Netrin/UNC-6 homologs. *Neuron, 17*(2), 217-228.

Hedgecock, E. M., Culotti, J. G., & Hall, D. H. (1990). The *unc-5, unc-6*, and *unc-40* genes guide circumferential migrations of pioneer axons and mesodermal cells on the epidermis in *C. elegans*. *Neuron, 4*(1), 61-85.

Hilliard, M. A., & Bargmann, C. I. (2006). Wnt signals and frizzled activity orient anterior-posterior axon outgrowth in *C. elegans. Developmental Cell*, 10(3), 379-390.

Hobert, O. (2002). PCR fusion-based approach to create reporter gene constructs for expression analysis in transgenic *C. elegans*. *BioTechniques, 32*(4), 728-730.

Hobert, O. (2010). Neurogenesis in the nematode caenorhabditis elegans. *WormBook : The Online Review of C.Elegans Biology, *, 1-24.

Hong, K., Hinck, L., Nishiyama, M., Poo, M. M., Tessier-Lavigne, M., & Stein, E. (1999). A
ligand-gated association between cytoplasmic domains of UNC5 and DCC family receptors
converts netrin-induced growth cone attraction to repulsion. *Cell*, 97(7), 927-941.

Hsu, T. Y., & Wu, Y. C. (2010). Engulfment of apoptotic cells in *C. elegans* is mediated by
integrin alpha/SRC signaling. *Current Biology : CB, 20*(6), 477-486.

Ishii, N., Wadsworth, W. G., Stern, B. D., Culotti, J. G., & Hedgecock, E. M. (1992). UNC-6, a
laminin-related protein, guides cell and pioneer axon migrations in *C. elegans*. *Neuron, 9*(5),
873-881.

Keleman, K., & Dickson, B. J. (2001). Short- and long-range repulsion by the drosophila Unc5
netrin receptor. *Neuron*, 32(4), 605-617.

Killeen, M., Tong, J., Krizus, A., Steven, R., Scott, I., Pawson, T., et al. (2002). UNC-5 function
requires phosphorylation of cytoplasmic tyrosine 482, but its UNC-40-independent
functions also require a region between the ZU-5 and death domains. *Developmental
Biology, 251*(2), 348-366.

Killeen, M. T., & Sybingco, S. S. (2008). Netrin, slit and wnt receptors allow axons to choose the
axis of migration. *Developmental Biology, 323*(2), 143-151.

Kolodkin, A. L., Matthes, D. J., O'Connor, T. P., Patel, N. H., Admon, A., Bentley, D., et al.
(1992). Fasciclin IV: Sequence, expression, and function during growth cone guidance in
the grasshopper embryo. *Neuron, 9*(5), 831-845.

Lee, J., Li, W., & Guan, K. L. (2005). SRC-1 mediates UNC-5 signaling in *Caenorhabditis elegans*. *Molecular and Cellular Biology, 25*(15), 6485-6495.

Leung-Hagesteijn, C., Spence, A. M., Stern, B. D., Zhou, Y., Su, M. W., Hedgecock, E. M., et al. (1992). UNC-5, a transmembrane protein with immunoglobulin and thrombospondin type 1 domains, guides cell and pioneer axon migrations in *C. elegans*. *Cell, 71*(2), 289-299.

Li, W., Lee, J., Vikis, H. G., Lee, S. H., Liu, G., Aurandt, J., et al. (2004). Activation of FAK and src are receptor-proximal events required for netrin signaling. *Nature Neuroscience, 7*(11), 1213-1221.

Liu, G., Beggs, H., Jurgensen, C., Park, H. T., Tang, H., Gorski, J., et al. (2004). Netrin requires focal adhesion kinase and src family kinases for axon outgrowth and attraction. *Nature Neuroscience, 7*(11), 1222-1232.

MacNeil, L. T., Hardy, W. R., Pawson, T., Wrana, J. L., & Culotti, J. G. (2009). UNC-129 regulates the balance between UNC-40 dependent and independent UNC-5 signaling pathways. *Nature Neuroscience*, 12(2), 150-155.

Maskery, S., & Shinbrot, T. (2005). Deterministic and stochastic elements of axonal guidance. *Annual Review of Biomedical Engineering, 7*, 187-221.

Mrkusich, E. M., Osman, Z. B., Bates, K. E., Marchingo, J. M., Duman-Scheel, M., & Whitington, P. M. (2010). Netrin-guided accessory cell morphogenesis dictates the dendrite orientation and migration of a *Drosophila* sensory neuron. *Development (Cambridge, England), 137*(13), 2227-2235.

Murai, K. K., & Pasquale, E. B. (2003). 'Eph'ective signaling: Forward, reverse and crosstalk. *Journal of Cell Science, 116*(Pt 14), 2823-2832.

Nakao, F., Hudson, M. L., Suzuki, M., Peckler, Z., Kurokawa, R., Liu, Z., et al. (2007). The PLEXIN PLX-2 and the ephrin EFN-4 have distinct roles in MAB-20/Semaphorin 2A signaling in *Caenorhabditis elegans* morphogenesis. *Genetics, 176*(3), 1591-1607.

Naqvi Z (2010). Identification of a novel gene altered in the RQ1 mutant strain affecting motor axon migration in *C. elegans*. Masters thesis, Ryerson University library, Toronto.

Palmer, A., & Klein, R. (2003). Multiple roles of ephrins in morphogenesis, neuronal networking, and brain function. *Genes & Development, 17*(12), 1429-1450.

Pan, C. L., Howell, J. E., Clark, S. G., Hilliard, M., Cordes, S., Bargmann, C. I., et al. (2006). Multiple wnts and frizzled receptors regulate anteriorly directed cell and growth cone migrations in *Caenorhabditis elegans. Developmental Cell*, 10(3), 367-377.

Quinn, C. C., Pfeil, D. S., Chen, E., Stovall, E. L., Harden, M. V., Gavin, M. K., et al. (2006). UNC-6/netrin and SLT-1/slit guidance cues orient axon outgrowth mediated by MIG-10/RIAM/lamellipodin. *Current Biology : CB, 16*(9), 845-853.

Raich, W. B., Moran, A. N., Rothman, J. H., & Hardin, J. (1998). Cytokinesis and midzone microtubule organization in *Caenorhabditis elegans* require the kinesin-like protein ZEN-4. *Molecular Biology of the Cell, 9*(8), 2037-2049.

Roy, P. J., Zheng, H., Warren, C. E., & Culotti, J. G. (2000). Mab-20 encodes semaphorin-2a and is required to prevent ectopic cell contacts during epidermal morphogenesis in *Caenorhabditis elegans*. Development (Cambridge, England), 127(4), 755-767.

Serafini, T., Kennedy, T. E., Galko, M. J., Mirzayan, C., Jessell, T. M., & Tessier-Lavigne, M. (1994). The netrins define a family of axon outgrowth-promoting proteins homologous to *C. elegans* UNC-6. *Cell, 78*(3), 409-424.

Shakir, M. A., Jiang, K., Struckhoff, E. C., Demarco, R. S., Patel, F. B., Soto, M. C., et al. (2008). The Arp2/3 activators WAVE and WASP have distinct genetic interactions with rac GTPases in *Caenorhabditis elegans* axon guidance. *Genetics, 179*(4), 1957-1971.

Shaw, G., & Bray, D. (1977). Movement and extension of isolated growth cones. *Experimental Cell Research, 104*(1), 55-62.

Siddiqui, S. S. (2002). Metazoan motor models: Kinesin superfamily in *C. elegans*. *Traffic (Copenhagen, Denmark), 3*(1), 20-28.

Su, M., Merz, D. C., Killeen, M. T., Zhou, Y., Zheng, H., Kramer, J. M., et al. (2000). Regulation of the UNC-5 netrin receptor initiates the first reorientation of migrating distal tip cells in *Caenorhabditis elegans*. *Development (Cambridge, England), 127*(3), 585-594.

Sybingco S (2008). Identification and analysis of novel mutants exhibiting defects in pioneer axon guidance in *C. elegans*. Masters thesis, York University library, Toronto.

Tessier-Lavigne, M., & Goodman, C. S. (1996). The molecular biology of axon guidance. *Science (New York, N.Y.), 274*(5290), 1123-1133.

Tong, J., Killeen, M., Steven, R., Binns, K. L., Culotti, J., & Pawson, T. (2001). Netrin

stimulates tyrosine phosphorylation of the UNC-5 family of netrin receptors and induces

Shp2 binding to the RCM cytodomain. *The Journal of Biological Chemistry, 276*(44),

40917-40925.

Tran, T. S., Kolodkin, A. L., & Bharadwaj, R. (2007). Semaphorin regulation of cellular

morphology. *Annual Review of Cell and Developmental Biology, 23*, 263-292.

Tsuboi, D., Qadota, H., Kasuya, K., Amano, M., & Kaibuchi, K. (2002). Isolation of the

interacting molecules with GEX-3 by a novel functional screening. *Biochemical and

Biophysical Research Communications, 292*(3), 697-701.

Wadsworth, W. G. (2002). Moving around in a worm: Netrin UNC-6 and circumferential axon

guidance in *C. elegans*. *Trends in Neurosciences, 25*(8), 423-429.

Wang, X., Roy, P. J., Holland, S. J., Zhang, L. W., Culotti, J. G., & Pawson, T. (1999). Multiple

ephrins control cell organization in *C. elegans* using kinase-dependent and -independent

functions of the VAB-1 eph receptor. *Molecular Cell, 4*(6), 903-913.

White, J. G., Southgate, E., Thomson, J. N., & Brenner, S. (1986). The structure of the nervous

system of the nematode *C. elegans*. *Philosophical Transactions of the Royal Society of

London - Series B: Biological Sciences, 314*(1165), 1-340.

Wong, J. T., Yu, W. T., & O'Connor, T. P. (1997). Transmembrane grasshopper semaphorin I

promotes axon outgrowth in vivo. *Development (Cambridge, England), 124*(18), 3597-3607.

Zallen, J. A., Yi, B. A., & Bargmann, C. I. (1998). The conserved immunoglobulin superfamily member SAX-3/Robo directs multiple aspects of axon guidance in *C. elegans. Cell*, 92(2), 217-227.

Zheng, H., Coudiere, L., Camia, C., Colavita, A., Culotti, J. G., & Merz, D. C. (2007). *C. elegans seu-1* encodes novel nuclear proteins that regulate responses to UNC-6/netrin guidance cues. *Developmental Biology, 310*(1), 44-53.